

TOPICAL REVIEW • OPEN ACCESS

4D printing: a cutting-edge platform for biomedical applications

To cite this article: Moqaddaseh Afzali Naniz *et al* 2022 *Biomed. Mater.* **17** 062001

View the [article online](#) for updates and enhancements.

You may also like

- [Triple shape memory polymers by 4D printing](#)
M Bodaghi, A R Damanpack and W H Liao
- [Modern concepts and application of soft robotics in 4D printing](#)
S Bharani Kumar, S D Sekar, G Sivakumar *et al.*
- [Enhanced multimaterial 4D printing with active hinges](#)
Saeed Akbari, Amir Hosein Sakhaei, Kavin Kowsari *et al.*



Breath Biopsy® OMNI®

The most advanced, complete solution for global breath biomarker analysis

TRANSFORM YOUR RESEARCH WORKFLOW



Expert Study Design & Management



Robust Breath Collection



Reliable Sample Processing & Analysis



In-depth Data Analysis



Specialist Data Interpretation

Biomedical Materials



TOPICAL REVIEW

4D printing: a cutting-edge platform for biomedical applications

OPEN ACCESS

RECEIVED
12 April 2022

REVISED
29 June 2022

ACCEPTED FOR PUBLICATION
31 August 2022

PUBLISHED
26 September 2022

Original content from this work may be used under the terms of the [Creative Commons Attribution 4.0 licence](https://creativecommons.org/licenses/by/4.0/).

Any further distribution of this work must maintain attribution to the author(s) and the title of the work, journal citation and DOI.



Moqaddaseh Afzali Naniz¹ , Mohsen Askari^{2,3} , Ali Zolfagharian⁴ , Mehrdad Afzali Naniz⁵ and Mahdi Bodaghi^{2,*}

¹ Graduate School of Biomedical Engineering, University of New South Wales (UNSW), Sydney, NSW 2052, Australia

² Department of Engineering, School of Science and Technology, Nottingham Trent University, Nottingham NG11 8NS, United Kingdom

³ Department of Textile Engineering, School of Material Engineering & Advanced Processes, Amirkabir University of Technology, Tehran, Iran

⁴ School of Engineering, Deakin University, Geelong, Victoria 3216, Australia

⁵ School of Medicine, Shahid Beheshti University of Medical Sciences, Tehran, Iran

* Author to whom any correspondence should be addressed.

E-mail: mahdi.bodaghi@ntu.ac.uk

Keywords: 4D printing, biomedical application, drug delivery, tissue engineering, medical devices, soft robotics

Abstract

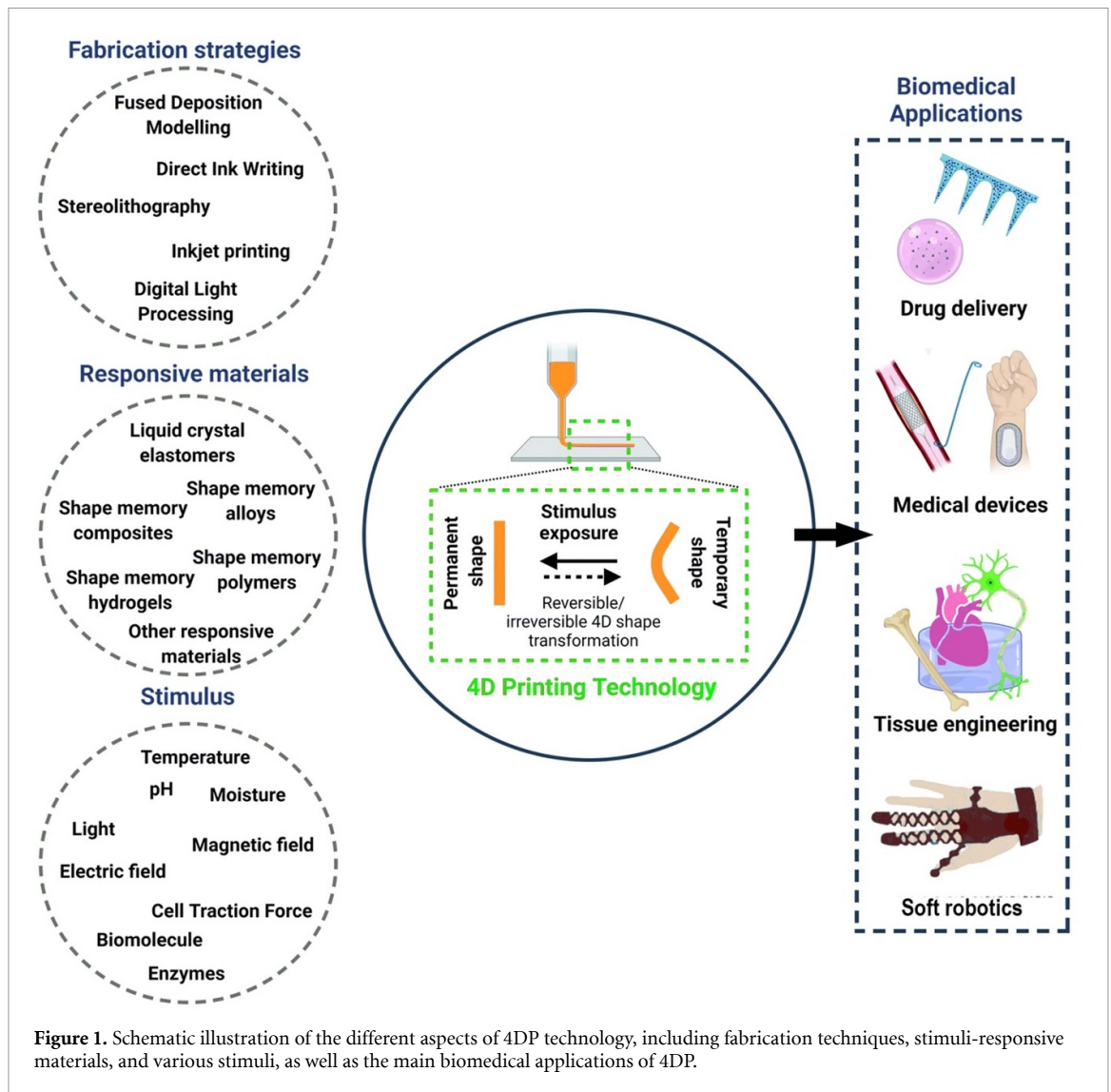
Nature's materials have evolved over time to be able to respond to environmental stimuli by generating complex structures that can change their functions in response to distance, time, and direction of stimuli. A number of technical efforts are currently being made to improve printing resolution, shape fidelity, and printing speed to mimic the structural design of natural materials with three-dimensional printing. Unfortunately, this technology is limited by the fact that printed objects are static and cannot be reshaped dynamically in response to stimuli. In recent years, several smart materials have been developed that can undergo dynamic morphing in response to a stimulus, thus resolving this issue. Four-dimensional (4D) printing refers to a manufacturing process involving additive manufacturing, smart materials, and specific geometries. It has become an essential technology for biomedical engineering and has the potential to create a wide range of useful biomedical products. This paper will discuss the concept of 4D bioprinting and the recent developments in smart materials, which can be actuated by different stimuli and be exploited to develop biomimetic materials and structures, with significant implications for pharmaceuticals and biomedical research, as well as prospects for the future.

1. Introduction

As a novel fabrication technology, three-dimensional printing (3DP) has led to the creation of customized biomedical devices such as stents [1, 2], implants [3–8], prosthetics [9, 10], and surgical tools [11] with unprecedented spatial resolution and design freedom. Moreover, 3D bioprinting was adapted from traditional 3DP technologies in order to construct biological constructs directly encapsulating cells into tissues such as the liver, heart, and blood vessels [12–14]. Using 3DP in biomedical applications allows for the customization and personalization of tissues, drugs, and medical products. Furthermore, it is less costly and faster than traditional manufacturing methods, which are usually employed in the biomedical field [15, 16].

A number of biomedical applications, however, require dynamic shape change, which cannot be achieved by conventional 3DP technologies [17]. Though 3DP is able to create heterogeneous tissues and organs using biomaterials and living cells [18], static 3D-printed structures cannot match native tissue dynamics and cannot satisfy the functional requirements of applications [19, 20]. The dynamic nature of biological tissues and their constantly changing shape require more advanced fabrication techniques [21, 22].

In order to meet this requirement, four-dimensional printing (4DP) has been introduced by extending 3D space to the fourth dimension of time [23, 24]. Combining the fourth dimension, time, allows continued control over the development of 3D-printed biomaterials and bioinks, enabling the



production of biomimetic tissues from the printed constructs to be pre-programmed and adjusted to achieve more native-like results [25, 26]. Thanks to 4DP, biomedical engineering has been given a new avenue. There have been numerous applications of 4DP in various academic fields and industries, including the biomedical area, where it is often referred to as 4D bioprinting [27–29]. A 4D bioprinting technique is used to create 3D dynamic structures that can change shape or function over time based on stimuli [30].

Smart designs and smart materials are necessary components for 4DP in order to achieve stimuli-responsive behaviours. As for smart designs, 4D-printed structures must be pre-programmed in computer-aided design (CAD) carefully by anticipating the time-dependent deformation of 3D objects [31, 32]. Materials which respond to external stimuli to change its geometry or properties are defined as smart materials [29]. Stimuli can be in the form of temperature, moisture, pH, light, pressure, or magnetic field. A variety of smart materials have been

used for 4DP, including shape memory metal alloys, shape memory polymers, stimuli-responsive hydrogels, dielectric elastomers, and smart nanocomposites (figure 1) [32–34].

While there have been tremendous advances in 3DP and now 4D bioprinting is seen as a next-generation printing technique capable of fabricating shape-transformable tissue-like structures, many limitations remain. Up to now, reports on 4D bioprinting have been limited due to the difficulty of developing appropriate smart biomedical materials containing living cells for printing. While this field is still in its early stage and only a few articles have been published, they clearly rank among the most remarkable developments and possibilities in the field of biofabrication [35–42].

Throughout this paper, we provide a comprehensive overview of 4DP and its applications in the tissue engineering, medical devices, soft robotics, and drug delivery systems. We provide our analysis of the challenges and potential future developments for 4DP in biomedical engineering, as well as our views on

possible future developments. This paper can contribute to an understanding of 4DP's current status and potential directions in biomedical engineering and pharmaceuticals.

2. Materials, methods, and technologies used in 4DP processes

2.1. Active/smart materials

4DP materials are generally referred to as Smart Materials because they have the capability to change their properties over time [35]. In the field of smart materials for 4DP, materials are synthesized according to their reactions to external stimuli, thereby developing a deformation mechanism. In addition to responding to external stimuli, they have the ability to self-assemble, self-heal, remember their shapes, and have self-reproducing capabilities [43]. Among the different types of smart materials available are shape memory polymers, electro-responsive polymers, magnetic shape memory alloys, smart organic polymers, shape memory alloys, temperature responsive polymers, photo-responsive polymers, and electroactive polymers. Based on the environment or external stimuli they respond to, 4DP materials can be categorized [20].

On the basis of their response to stimuli, here are the most common categories of smart materials employed in 4DP techniques.

2.1.1. Moisture responsive materials: hydrogels

This category includes materials that react with moisture or water when in contact. Such materials are common among researchers, since water is readily available and can be used in various applications. Hydrogels, because of their strong reaction to water, is one of the most intelligent materials in this category. The ability to drastically alter the volume makes them more popular in 4DP. Combining these with a second polymer network increases the strength and is used in the biomedicine. Furthermore, hydrogels are versatile in terms of printing. They are capable of folding, bending, stretching, and geometrical expansion. However, the only drawback is their slow reverse reaction, so one must wait hours before they shrink and dry. It is necessary to program the hydrogels to add anisotropy to their swelling in order to overcome this problem [33, 44].

2.1.2. Thermo-responsive materials

Thermo-responsive materials are those that react to temperature. Shape change effects and shape memory effects (SMEs), are primarily responsible for the shape changes in these materials in response to thermo stimuli. SME is the process of restoring original shape to a deformed (plastic) material by the use of external stimuli. Shape-memory materials (SMMs) are smart materials that show the SME effect. Generally, SMMs can be classified into shape memory alloys (SMAs),

shape memory polymers (SMPs), shape memory hybrids, shape memory ceramics, and shape memory gels. Depending on the number of shape transformations, SMMs can be divided into one-way, two-way, and three-way materials. A one-way SMM cannot regain its original shape after deformation whereas a two-way or three-way SMM can regain its original shape after deforming into a temporary shape via intermediate shapes [45, 46].

2.1.3. Photo-responsive materials

The light also stimulates the deformation of smart materials indirectly. In smart materials, absorbing light is the cause of the heating phenomenon that is created when exposed to light. The deformation of smart materials occurs as a result of heat, so a shape change occurs in the photo-responsive material. Because light does not directly cause change, it acts as an indirect stimulus [47, 48].

2.1.4. Electro-responsive materials

As with light, electricity is also indirectly modulated, since it has been shown to create a heating effect when passed through a material that has a resistive nature. So, materials that respond to electrical currents by deforming due to their responsiveness are called electro-responsive materials. Their capability for remote actuation when they are triggered by external electric fields is one of their most remarkable attributes. An important and robust way to actuate small objects is with this feature. Hence, these are more feasible than other stimuli such as direct heating, as they are easy to use, fast actuation/reaction times, and compatible with biological environments [49].

2.1.5. Magneto-responsive materials

Likewise, magnetic fields and magnetic energy are indirect stimuli that can cause smart materials to deform. Magneto-responsive materials are materials that can deform in response to magnetic energy, which makes them suitable for printing 4D structures. The remote actuation capabilities of these materials make them particularly useful when actuating small objects. There is huge potential in the use of magneto-responsive materials for 4DP metal and polymer structures, however, the size of the print has to be fairly light so that it will respond to magnetic fields [50, 51].

2.1.6. pH-responsive materials

Smart materials respond to changes in pH and undergo shape and volume changes as a result of those changes. In response to pH changes, they deform in shape, making them suitable for 4DP. Polyelectrolytes, which have an ionizable side group, have been used in 4DP because of their pH-responsive polymer properties. Upon proton release, a polymer chain stretches due to electrostatic repulsion, resulting in

deformation of the structure. Upon proton acceptance, the structure is neutralized [52, 53].

2.1.7. Piezoelectric materials

Piezoelectric materials capable of converting mechanical and electric energy have been widely utilized in biomedical engineering due to their unique electro-mechanical and acoustic properties. As they can deform under the influence of a mechanical force, they can be used for 4DP applications. There is a simple mechanism: the stress will be applied, and then charges will be produced, leading to changes in the structure (as the charge can cause deformation) [23, 54].

2.2. 4DP techniques

A few modifications are necessary to adapt former 3DP techniques to 4DP of shape memory polymer/smart materials. By adding an air circulation system to existing fused deposition modeling (FDM) 3DP techniques, SMP can be cooled below low glass transition temperatures. This will enable SMP to achieve the shape change required per prediction or for the appropriate application. After minor changes, other 3DP techniques such as stereo lithography (SLA), electron beam melting (EBM), and inkjet printing may also be used [45, 55].

2.2.1. FDM

Among all of the methods, this is the most popular due to its feasibility. This technique is characterized by the extrusion of a material into a substrate and its subsequent hardening. *X*- and *Y*-axis movement of the nozzle is enabled by a motor. An already printed layer is printed over by moving the nozzle in the *Z* axis upwards. It is done in this way until a final structure is made. Because of its cost-effectiveness and ease of maintenance, FDM is widely used in 4DP, and research is currently being conducted to make it more effective and compatible with new materials. It is easy to fabricate self-coiling and self-folding metamaterials using FDM. Updates have made FDM capable of printing new materials [56, 57].

2.2.2. Direct ink writing (DIW)

Using this extrusion-based procedure, viscoelastic inks are deposited under high pressure through nozzles to create dynamic, smart structures. This technique has been used to manufacture biodegradable scaffolds for tissue engineering applications. Self-healing, highly stretchable SMPs were printed using UV assisted DIW for biomedical repair devices and wound healing applications [58].

2.2.3. Inkjet printing

Inkjet printing, which is also called drop-on-demand (DOD) printing, was one of the first widely used methods of 3DP. With inkjet printing, ejection of

photo resin drops from a printhead is caused by pressure and voltage pulses; therefore, it is called DOD printing. Inkjet printing fluids typically contain UV-curable acrylate liquid, which solidifies instantly when exposed to UV light. As a second method of inkjet printing, a liquid binder is spread on the building platform using an inkjet printhead that moves freely in 2D. To deposit the second powder-liquid binder layer, the initial pattern is lowered. The entire powder-inkjet printing process is repeated several times to achieve the final product. As it is highly biocompatible, inkjet printing is majorly used for bioprinting of living cells in the biomedical field. Powder-based inkjet 3DP offers advantages such as flexibility in terms of selecting materials and processing them at room temperature. A tenth of a micrometer spatial resolution is achievable using inkjet technology. Contamination may occur as a result of the binder used during deposition, which is the main disadvantage of this process. Furthermore, since inkjet printing requires low-viscosity formulations, it is limited [59, 60].

2.2.4. SLA

SLA is another well-known 3DP technique that uses light (laser) emitted at a variety of frequencies in order to solidify liquid polymers and resins. This method involves curing a liquid resin with lasers to form a 3D structure layer by layer. To put it simply, the reaction occurs when light falls on the material, which causes the resin molecules to bond together, forming a solid structure. When cured, photopolymers become gels and then cross-link into solid polymers. SLA can produce structures with an elongation of up to 80% in comparison to other methods. It is commonly used to fabricate difficult and complex structures. Compatible materials have also been developed for SLA printing [61]. Photo cross-linking hydrogels and photocurable resins SMPs or liquid-crystal polymers (LCPs) are among the materials commonly 4D printed with SLA. In comparison with extrusion printing technologies, SLA's main advantages are its high printing resolution and excellent surface quality [62].

2.2.5. Digital light processing (DLP)

By using light as a crosslinking agent, DLP printing has proved to be a valuable tool for quickly fabricating complex 3D and 4D constructs. This method can achieve high print resolution, high printed shape-to-design fidelity, and provides a choice of printing materials. As opposed to SLA, DLP uses a digital light pattern instead of a scanning laser beam to cure liquid resin in a reservoir in about a second per layer. A DLP printer can reach high printing speeds, on the order of multiple times faster than what is possible with SLA because it uses a surface-projection based fabrication method [63, 64].

3. An up-to-date insight to the opportunities for different biomedical applications

In the following paragraphs, we will discuss the main applications of 4DP in the biomedical field, i.e. tissue engineering, medical devices, soft robotics, and drug delivery systems, citing some of the most significant studies in recent literature.

3.1. Tissue repair and regeneration

Tissue engineering and regenerative medicine is an interdisciplinary field that integrates cell-based therapies and bioactive and porous materials to replace or restore damaged tissues and organs [65]. In tissue engineering, three elements must be in harmony: (a) matrix (scaffold), (b) cells (stem cells or primary lineages), and (c) signals (mechanical, physical, electrical, and/or molecules such as proteins, peptides, and cytokines). As a key factor, scaffolds provide physical and structural support for cell growth and differentiation, as well as transport of nutrients [66]. The morphology and chemical composition of the matrix should mimic those of the extracellular matrix, simulating an extracellular environment that encourages cell-material contact [67]. Pore size and porosity rate directly impact tissue formation inside 3D scaffolds, so these factors must be tailored for tissue restoration. These characteristics are essential in providing an adequate oxygen supply to promote angiogenesis [68]. The tissues are highly plastic, non-static, and have unique functions suitable for dynamic changes in the human body. While conventional 3D-printed structures could have specific shapes, architectures, or cells, they cannot show dynamic processes. Given this, 4D bioprinting essentially meets the biomedicine requirement [69]. Figure 2 demonstrates how 4DP can be applied to tissue regeneration. An overview of recent applications of 4DP in tissue engineering can be found in Table 1.

The most common materials for 4D bioprinting in tissue engineering are hydrogels and SMPs. A variety of SMPs have been investigated for creating shape-morphing biomedical products. Wang *et al* employed a temperature-responsive polymer (poly(D, L-lactide-co-trimethylene carbonate)) to create porous tissue engineering scaffolds using cryogenic 3D dispensing [71]. In this study, the microstructure of constructs was studied as a function of water content in emulsions. As a result of their exceptional shape-morphing ability and injectability, the scaffolds hold a great deal of potential for minimally invasive implantation. Furthermore, growth factors were loaded into the scaffolds *in situ* and showed sustained release after 30 d. Furthermore, some SMPs have been processed via 4DP into smart tissue engineering scaffolds that undergo shape evolution when heated, including methacrylate polycaprolactone [72] and soybean oil epoxidized acrylate (SOEA) [73].

Due to the harsh situations in the preprogramming process with stimuli such as temperature [74], most studies about the *in vitro* biomedical application of 4D bioprinting have been performed by seeding cells on pre-prepared scaffolds consisting of smart materials. The *in vitro* results of the cell-seeded 4D construct exhibited good cytocompatibility after fulfillment of the fabrication and preparation procedures, although it was still required to assess the cytotoxicity or cell damage during deformation or shape recovery [73, 74].

According to the published study on 4D bioprinting, several natural hydrogels are combined with living cells to produce bioprinting inks, which can be exploited to print 3D dynamic structures with living cells and strategically control their cross-linking degree gradient across the thickness or plane of these structures. In response to water, these 4D-bioprinted constructs can alter their forms based on hydrogels' anisotropic swelling and shrinking properties. For instance, living cells were incorporated into 4D-bioprinted dynamic structures using photo-crosslink silk fibroin, gelatin methacryloyl (GelMA), and hyaluronic acid methacryloyl [75, 76]. The use of 3D bioprinting of a cell-laden matrix on a shape memory substrate to create a biphasic structure with living cells is another effective method for achieving 4D bioprinting. For instance, Luo *et al* created a bilayer construct consisting of an alginate/polydopamine shape-morphing layer [exhibiting near-infrared (NIR)-induced dehydration of alginate] and a cell-laden GelMA layer [77].

Beyond shape-changing constructs, structures with functional changes are anticipated that can undergo post-fabrication maturation to attain distinct functions that are similar to those of natural tissues. The development of 3D-printed objects composed of cell spheroids and organoids has recently been demonstrated [78–80]. A few studies on treating cells as applied stimuli or smart materials are in the literature. The first example is a famous study on the self-folding effect utilizing cell traction force (CTF) as a stimulus for SMEs [81]. Diverse patterns, intervals, and joints of cell-seeded microplates were employed to control the development of various shapes of 3D cell-laden constructs in a procedure defined as cell origami.

3.1.1. Vascular regeneration

Using 4D bioprinting can alleviate a substantial challenge in fabricating functional tissues via 3DP, i.e. vascularization. A 4D-printed self-folding polymer can be employed to construct blood vessels capable of encapsulating blood cells, which, once wet, deform into a tubelike structure [82]. Multiple self-folding structures can currently be manufactured with photo-crosslink hydrogels or SMPs through 4D bioprinting [83]. 4D-bioprinted hydrogels can be transformed into microvascular

Table 1. Overview of 4DP applications in tissue engineering.

| Applications | Stimuli | Materials ^a | Cells ^b | Printing techniques ^c | Reference |
|-------------------------------------|---|--|---|--|-----------|
| 3D cell culture, histological study | Temperature | PEGDA, Bis-EMA | Human neural progenitor cell | PμSLA | [121] |
| 3D cell culture (neural) | Temperature | PVA (microstructured mold preparation), PMMA (microwell imprinting mold) BDE, PBE, and DA (4D ink) | Mouse NSCs | FDM, SLA, replica molding and imprinting | [102] |
| Vascular tissue engineering | Water | Alg-MA, HA-MA | D1 cells | Extrusion | [75] |
| Vascular tissue engineering, stent | Temperature | PGDA | — | Extrusion | [122] |
| Cardiac tissue engineering | Temperature | SOEA | Human MSCs | PSTS | [92] |
| Cardiac tissue engineering | Water (solvent-induced stress relaxation) | GelMA and PEGDA | Human (iPSC-CMs), humanMSCs, HUVECs | SLA | [94] |
| Cardiac tissue engineering | NIR-induced photothermal effects | PEGDA (mold preparation) BDE, PBE, DA, and graphene nanoplatelets (4D ink) | Human (iPSC-CMs), humanMSCs, HUVECs | DLP and replica molding | [93] |
| Neural tissue engineering | Temperature and NIR- induced photothermal effects | PVA (mold preparation), BDE, PBE, DA, and graphene nanoplatelets (4D ink) | Mouse NSCs | FDM, extrusion, and replica molding | [95] |
| Neural tissue engineering | Solvent (water/ethanol), temperature | SOEA (with/without graphene) | Human MSCs | SLA | [101] |
| Neural tissue engineering | Magnetolectric | 4-HBA, PU-EO-PO monomer, and electro-magnetized carbon porous nanocookies | PC12 cells | DLP | [123] |
| Bone/ cartilage tissue engineering | Water | Oxidized Alg-MA | NIH-3T3 cells, human adipose-derived stem cells | Extrusion | [124] |
| Bone tissue engineering | Water, pH, Calcium ions | Oxidized Alg-MA and GelMA | Human MSCs | Extrusion | [125] |
| Bone tissue engineering | Temperature | PU, superparamagnetic iron oxide nanoparticles (combined with gelatin or PEO) | Human MSCs | LTDM | [126] |
| Bone tissue engineering | NIR-induced photothermal effects | BPNS, β-TCP, and p(DLLA-TMC) | Rat MSCs | Extrusion | [115] |

(Continued.)

Table 1. (Continued.)

| Applications | Stimuli | Materials ^a | Cells ^b | Printing techniques ^c | Reference |
|----------------------------|----------------------------------|---|-------------------------------------|----------------------------------|-----------|
| Bone tissue engineering | Temperature | Poly (propylene fumarate) | — | DLP | [127] |
| Bone tissue engineering | Water, Temperature | PCLDA-2000 and PCLDA-10 000 (micropatterned SMP layer) HEA, PCLDA-2000, and SPMA (hydrogel layer) | Rat MSCs | DLP | [116] |
| Bone tissue engineering | Thrombin, alkaline phosphatase | PEGDA (700) | NIH-3T3 cells | DLP | [128] |
| Bone tissue engineering | Temperature | Castor oil and PCL triol | Human MSCs | Extrusion | [129] |
| Trachea tissue engineering | Magnetic field | PLA, Fe ₃ O ₄ nanoparticles | — | Extrusion | [130] |
| Trachea tissue engineering | Water and NaCl | Sil-MA | Human/rabbit chondrocytes and TBSCs | DLP | [76] |
| Muscle tissue engineering | Temperature | PCL triol and poly(hexamethylene diisocyanate)—coated PCL | Human MSCs | FDM | [131] |
| Muscle tissue engineering | Calcium ions | Alg-MA and PCL | C2C12 cells | Extrusion, MEW | [87] |
| Muscle tissue engineering | Water | HA-MA and PCL-PU | C2C12 cells | Extrusion, MEW | [132] |
| Tissue engineering | Water | GelMA (top layer) Carboxylated GelMA (bottom layer) PEI/HA/Alg/Alg-gelatin (sacrificial layer) | HUVEC | Inkjet | [86] |
| Tissue engineering | NIR-induced photothermal effects | Alg and polydopamine(for shape morphing) Alg and GelMA (for cell encapsulation) | 293 T HEK cells | Extrusion | [77] |
| Tissue engineering | Temperature | SOEA | Human MSCs | SLA | [73] |
| Tissue engineering | Temperature | Collagen conjugated-polyether urethane (MM3520) | Human MSCs | Extrusion | [74] |
| Tissue engineering | Temperature | pAAm, pNIPAAm, Alg, and sugar particles | — | Extrusion | [133] |
| Tissue engineering | Water, temperature | HBC-MA | — | SLA | [134] |
| Tissue engineering | Temperature | Agarose, pAAm, and LAPONITE® | — | Inkjet | [135] |

(Continued.)

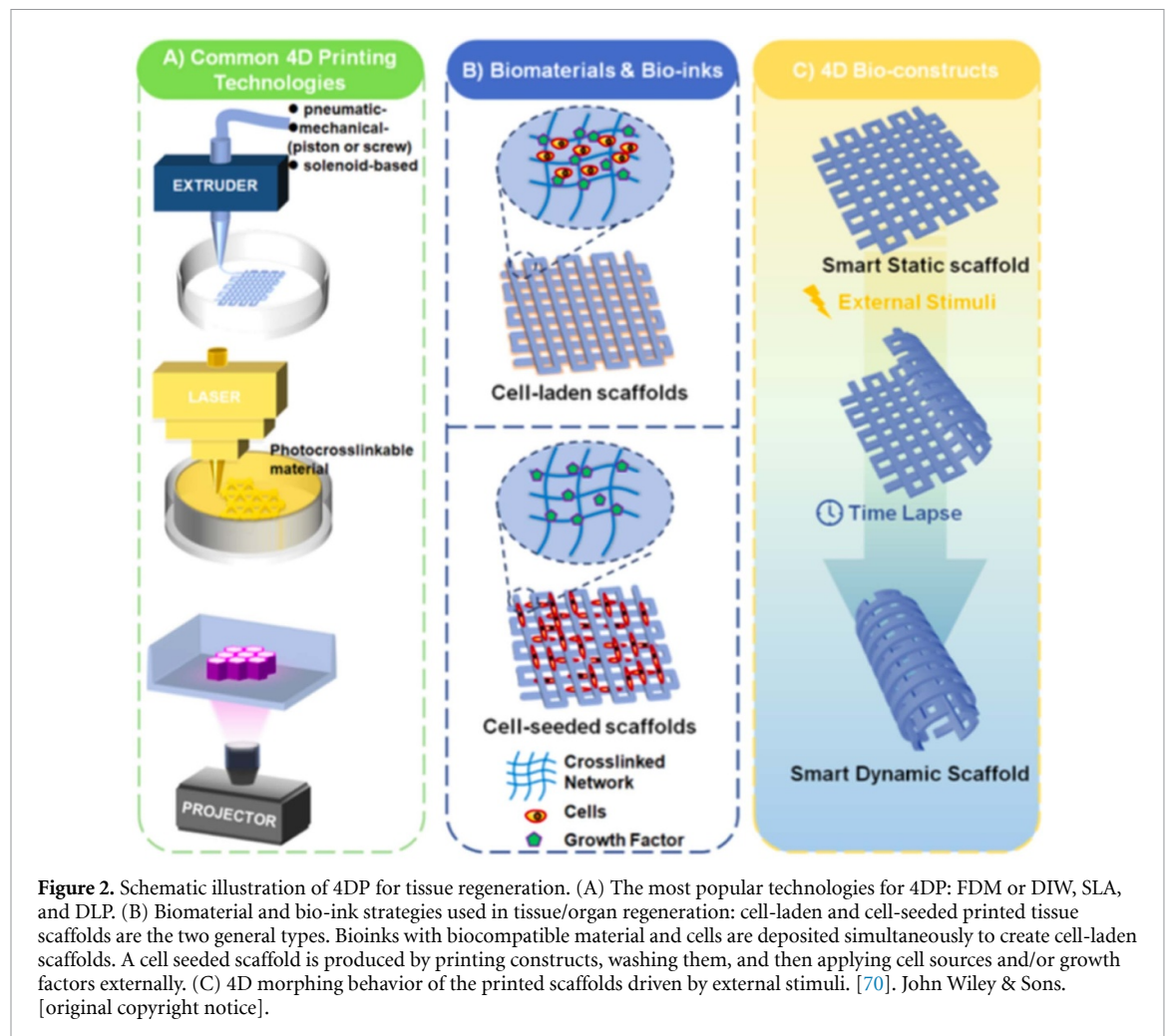
Table 1. (Continued.)

| Applications | Stimuli | Materials ^a | Cells ^b | Printing techniques ^c | Reference |
|--------------------|-------------|------------------------------------|--------------------|----------------------------------|-----------|
| Tissue engineering | Temperature | PLA | — | Extrusion | [136] |
| Tissue engineering | Water | PEGDA, HEMA, SPMA, AUD, and MEO2MA | — | SLA | [137] |

^a PEGDA: poly (ethylene glycol) diacrylate; Bis-EMA: bisphenol A ethoxylate dimethacrylate; PVA: polyvinyl alcohol; PMMA: polymethyl methacrylate; BDE: bisphenol A diglycidyl ether; PBE: poly(propylene glycol) bis(2-aminopropyl ether); DA: decylamine; Alg-MA: alginate methacrylate; SA: sodium alginate; HA-MA: methacrylated hyaluronic acid; PGDA: poly(glycerol dodecanoate) acrylate; SOEA: soybean oil epoxidized acrylate; 4-HBA: 4-Hydroxybutyl acrylate, PU-EO-PO: urethane–polyethylene glycol–polypropylene glycol; PU: Polyurethane; GelMA: gelatin–methacryloyl; PEO: poly(ethylene oxide); BPNS: black phosphorus nanosheets; β -TCP: β -tricalcium phosphate; p(DLLA–TMC): poly(lactic acid-co-trimethylene carbonate); HEA: hydroxyethylacrylate; PCL: poly(ϵ -caprolactone); Sil-MA: methacrylated silk; HA: hyaluronic acid; PEI: polyethyleneimine; pAAm: polyacrylamide; pNIPAAm: poly(N-isopropylacrylamide); HBC-MA: hydroxybutyl methacrylated chitosan; HEMA: hydroxyethyl methacrylate; SPMA: sulfopropyl methacrylate potassium; AUD: aliphatic urethane diacrylate; PLA: poly(lactic acid); MEO2MA: (2-methoxyethoxy) ethyl methacrylate.

^b NSCs: neuronal stem cells; MSCs: mesenchymal stem cells; Human (iPSC-CMs): human-induced pluripotent stem cell-derived cardiomyocytes; HUVECs: human umbilical vein endothelial cells; TBSCs: trophoblast stem cells; HEK: human embryonic kidney; BMP-2: bone morphogenetic protein-2.

^c P μ SLA: projection micro stereolithography; FDM: fused deposition modelling; SLA: stereolithography; PSTS: photolithographic–stereolithographic–tandem strategy; DLP: Digital Light Processing; LTDM: low-temperature deposition manufacturing.



scaffolds with 20–500 μm diameter by controlling the through-thickness cross-linking degree of photocrosslink hydrogels [75, 76, 84].

As a further benefit, vascular structures can be produced in small or large diameters and can self-fold from a 2D planar shape into a 3D hollow tube when stimuli are applied. Upon heating to human body temperature, a printed planar SMP scaffold can self-fold into a vascular scaffold with a diameter of several micrometers to centimeters, which allows homogeneous cellular spreading, which is difficult to achieve in 3DP [85].

Cui *et al* used inkjet printing to generate bilayer micropatterned structures on substrates treated with sacrificial coatings [86]. Specifically, the upper and lower layers contain GelMA and its carboxylated form, respectively. The swelling rates of these materials differ upon exposure to water, i.e. GelMA swells more slowly than carboxylated GelMA, thus resulting in a shape change, from planar to curved. The sacrificial layer allowed specific control over the timing of initiating self-folding, thereby forming self-folded microtubes that replicated human microvessels. Moreover, the sacrificial layer also determined the constructs' self-folding after printing, enabling the cultivation of human umbilical vein endothelial cells (HUVECs) during the early experimental stages.

To fabricate bi-layer scroll-like scaffolds with anisotropic topography, Constante *et al* employed a hybrid method that combined extrusion bioprinting of alginate methacrylate (Alg-MA) and melt-electrowriting of poly(ϵ -caprolactone) (PCL) fibres [87]. Combining these two techniques and materials enables the production of adaptive multiscale, multi-material constructs capable of self-folding when inflated. The authors could control the shape-morphing behaviour by adjusting the calcium ion concentration, media composition, and geometrical shape of the structure. The 4D-printed bi-layer scaffolds also showed superior viability, proliferation, and alignment of the C2C12 myoblasts.

3.1.2. Cardiac patches and valves

Heart tissue loses its regenerative abilities after myocardial infarction. New regenerative treatments for cardiovascular diseases are continuously being developed [88, 89]. Cardiac patches are innovative bioengineered scaffolds used to treat heart conditions. It is an effective technique to eliminate deficiencies and improve the mechanical strength of the infarcted area [90]. The architecture of cardiac scaffolds/patches must be curved and aligned to successfully attach to the surface of the heart to repair injured myocardial tissue [70]. In comparison to 3DP for cardiovascular regeneration, as explained in our previous review [91], 4DP has the capability of fabricating curved surfaces that are physiologically relevant, as well as incorporating dynamic mechanical stimulation.

Miao *et al* developed a 4D hierarchical micropatterned cardiac patch with smart SOEA inks employing an integrated SLA technique with photolithography [92]. The 4D functioning scaffolds show remarkable cell compatibility, and human mesenchymal stem cells (hMSCs) actively grow along the formed micropattern. Specifically, the aligned micropatterns developed by stereolithography could induce cell alignment and cardiomyogenic differentiation of hMSCs. By repeated self-folding and recovery, the 4D scaffold could be used as a myogenic bioreactor. hMSCs actively grow along the micropatterns formed by the 4D scaffolds, demonstrating remarkable cell compatibility (figure 3(A)). Specifically, the aligned micropatterns created by stereolithography could induce cardiomyogenic differentiation in human stem cells. This scaffold could be utilized as a myogenic bioreactor through repeated self-folding and recovery. Despite this, the process temperature still represented a harsh environment for living cells. Therefore, it is still unclear whether the whole shape recovery process could be used as a bioreactor.

In another study, Cui *et al* fabricated a 4D self-morphing cardiac patch with biomechanical adaptability via beam-scanning SLA [94]. In more detail, the printing process induced graded internal stresses that, after solvent-induced relaxation, enabled the patch to change from a flat 3D mesh design to a 4D wavy design. The specific design of combining a novel self-morphing 4D capability with an expanding microstructure has been demonstrated to enhance the patch's dynamic integration with the beating heart and the patch's biomechanical properties. *In vitro* studies under physiologically relevant mechanical stimulation showed that the patch with a wavy design, co-cultured with hMSCs, hiPSC-CMs, and HUVECs boosted vascularization and cardiomyocyte differentiation. Also, after three weeks from the implantation of the 4D-printed patches into a murine chronic (myocardial infarction) MI model, strong adhesion to the epicardium occurred, as well as increased cell engraftment and vascular infiltration.

Researchers are always on the lookout for creative and harmless stimuli that would enable better performance in 4DP. In particular, NIR light has gained popularity because of its non-invasiveness, high penetration, and capability to remotely control shape transformation [95, 96]. In this respect, Wang *et al* utilized 4D inks, formed of bisphenol A diglycidyl ether (BDE), poly(propylene glycol) bis(2-aminopropyl ether) (PBE), and decylamine (DA), and graphene nanoplatelets, to generate micropatterned nanocomposite structures to engineer cardiac tissues, as shown in figure 3(B) [93]. The procedure involved two steps; (a) 3DP of micropatterned poly(ethylene glycol) diacrylate (PEGDA) molds employing DLP and (b) extrusion filling of 4D inks into the molds to create final structures. NIR-induced

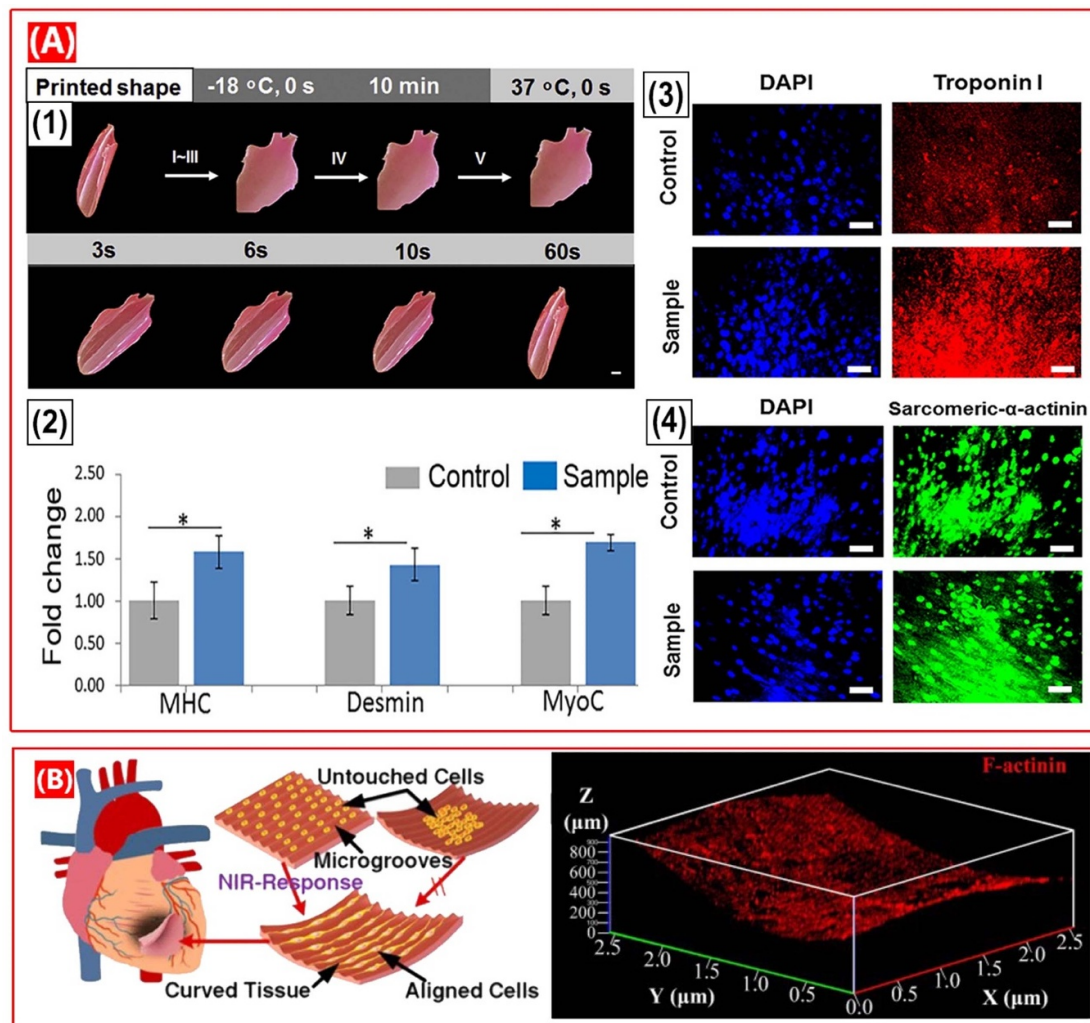


Figure 3. 4D-printed cardiac tissue scaffolds. (A) Shape memory effect and cardiomyogenic differentiation of hMSCs on 4D-fabricated scaffolds and controls. (1) Using a 4D-printed heart-shaped construct to demonstrate the shape memory process. Upon being placed in a 37 °C environment, the flat heart-shaped construct gradually recovered its original rolling shape. Scale bar, 2 mm. (2) The expression of MHC, desmin and MyoC was measured by qRT-PCR. (3) The expression of cardiac troponin I. (4) The expression of sarcomeric- α -actinin. Reproduced from [92]. © IOP Publishing Ltd. All rights reserved. (B) An illustration of a 4D-printed cardiac patch that is NIR-light-responsive and shows an immunofluorescent image of human induced pluripotent stem cell-derived cardiomyocytes (hiPSC-CMs) cells attached. Reprinted with permission from [93]. Copyright (2021) American Chemical Society.

photothermal effects caused the construct to change shape from flat to curved (mimicking the curved surface of myocardial tissue), emphasizing the potential for remote manipulation of the scaffold. Human iPSC-CMs, MSCs, and HUVECs were also cultivated on the scaffold. The 4D curved cardiac scaffold exhibited even cell alignment and superior myocardial maturation.

In the future, 4D bioprinting will be helpful in advancing *in vivo* investigations. In this case, structural changes in implanted structures will be necessary after printing due to environmental changes or CTFs [20, 97]. Accordingly, some researchers studied preoperative planning using 4D models for future applications of 4D bioprinting in surgery [98]. A high-resolution 4D flow model for cardiac tissue was developed and simulated, providing insights for additional optimization of surgical methods.

3.1.3. Neural scaffolds and conduits

One of the most challenging clinical issues in the world is the regeneration of nerve damage or defects caused by traumatic injury (including brain damage) and neurological disease (e.g. strokes, Alzheimer's disease, Parkinson's disease, multiple sclerosis, and Huntington's disease). In addition to the many possible neuroregenerative treatment strategies being studied currently, 3D bioprinted scaffolds have the distinct advantage of being highly customizable. This means that their structure mimics the native biological architecture of *in vivo* systems [99, 100]. The aim of this section is to demonstrate the unique characteristics of 4D-printed neural scaffolds, such as dynamic self-enturbulation and seamless integration, that have been recently designed for neural tissue engineering.

As one of the first to demonstrate remotely and dynamically controlled 4DP, Wang *et al* created a

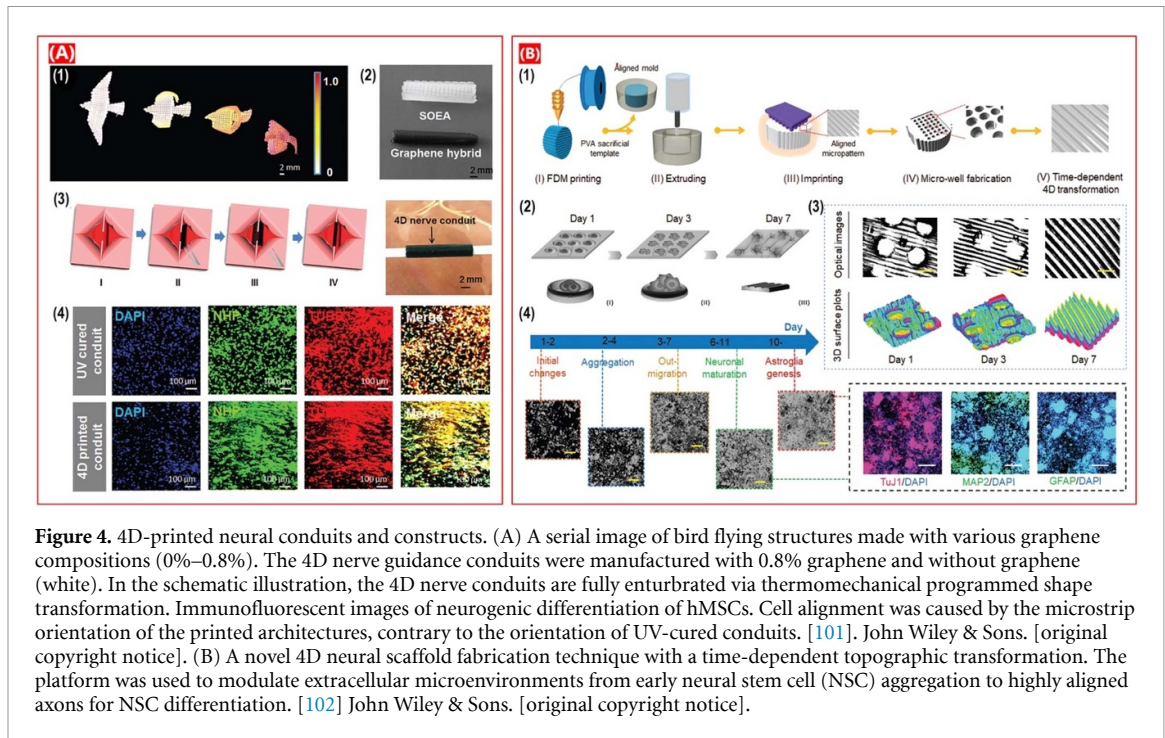


Figure 4. 4D-printed neural conduits and constructs. (A) A serial image of bird flying structures made with various graphene compositions (0%–0.8%). The 4D nerve guidance conduits were manufactured with 0.8% graphene and without graphene (white). In the schematic illustration, the 4D nerve conduits are fully entubrated via thermomechanical programmed shape transformation. Immunofluorescent images of neurogenic differentiation of hMSCs. Cell alignment was caused by the microstrip orientation of the printed architectures, contrary to the orientation of UV-cured conduits. [101]. John Wiley & Sons. [original copyright notice]. (B) A novel 4D neural scaffold fabrication technique with a time-dependent topographic transformation. The platform was used to modulate extracellular microenvironments from early neural stem cell (NSC) aggregation to highly aligned axons for NSC differentiation. [102] John Wiley & Sons. [original copyright notice].

photothermal graphene-based thermally responsive brain model [95]. NIR irradiation transformed the 4D scaffold from a short-term flat shape to its folded original shape. Besides, compared to pure epoxy scaffolds, the neural stem cell-laden constructs showed superior growth and differentiation of neural stem cells due to their conductive and optoelectronic properties.

Using a photocrosslinkable SOEA ink and an SLA, Miao *et al* developed a novel nerve guidance conduit that is temperature-sensitive [101]. Both the laser-induced graded internal stress and the SME can trigger the 4D plus reprogramming of structures. The developed nerve conduct exhibited excellent 4D shape transformation capabilities to provide a minimally invasive, surgical procedure with *in situ* shape activation, as seen in figure 4(A). The ability of the 4D-printed constructs to dynamically and seamlessly integrate into the stumps of a damaged nerve also indicated that they possessed good potential for neural tissue regeneration by exhibiting neural differentiation.

Recently, the same research group developed a 4D programmable medium for culturing NSCs by combining printing and imprinting techniques (i.e. fused deposition modelling (FDM), DIW, and SLA) to enhance dynamic cell growth and induce stem cell differentiation, as shown in figure 4(B) [102]. Results demonstrate that the 4D culture substrate shows a self-morphing time-dependent procedure that plays a vital role in controlling NSC behaviours and improves neuronal differentiation of NSCs. It means that the 4D shape transformation allowed axons to become highly aligned as cellular aggregates, replicating a microenvironment for neural tissue differentiation.

Unlike other tissue scaffolds or biomedical devices, 4D nerve grafts do not require large-scale or complex shape modifications. In fact, they go from plane to conduit in one step. Due to this, it will likely be more readily available commercially in the future.

3.1.4. Muscle tissue scaffolds

A human body's muscle makes up approximately half of its weight. All body movements involve muscle in some way since muscle tissue is dynamic and the only tissue to contract, or shorten [103]. There are three primary types of muscle tissue in the muscular system: skeletal, cardiac, and smooth. Each type has a unique structure and a distinct function [104]. In recent years, 3DP has gained popularity as a technology that can fabricate engineered muscles with heterogeneous properties and structures [105, 106]. It is, however, incapable of exhibiting any dynamic mechanical properties such as stretching or folding to respond to myogenic alignment and functional maturation. As a result, 4DP has become a viable option.

A novel hierarchical micropattern was created by Miao *et al* with a unique photolithographic-stereolithographic-tandem strategy (PSTS) and smart SOEA inks [92]. By applying an external stimulus to the surface-patterned scaffold, the 4D effect converts it into a pre-designed construct autonomously. According to the results, hMSCs grew strongly and were aligned along the micropatterns, forming a continuous cellular sheet. Immunofluorescence staining and qRT-PCR analysis confirmed cardiomyogenesis in hMSCs grown on the scaffolds, indicating that these scaffolds could be used for future tissue and organ regeneration procedures.

Moreover, Yang *et al* developed a system for cell-laden GelMA microfibres to enable cell alignment and promotion of myogenic differentiation using an electric field (EF) assisted cell-printing and 4DP approach [107]. Compared to the normally printed cell-laden structure, the electric field-induced cell alignment promoted significantly greater myotube formation, the formation of highly ordered myotubes, and enhanced maturation. An *in vitro* process was activated through voltage-gated calcium channels similar to the mechanism that governs muscle contraction *in vivo*. The results indicated that cells at medium density (15×10^6 cells ml^{-1}) are very aligned when treated with an EF (>0.4 kV cm^{-1}).

As discussed above, the alignment methods of 4D muscle scaffolds could be adapted to other tissues with a high degree of organization and anisotropy. For example, the use of EF in other non-printing methods has been widely applied for initiating cellular activity, such as migration, alignment, and differentiation. In particular, some electroactive cells, such as neurons and skeletal (or cardiac) muscle cells, may be mediated by electrical stimulation for their normal physiological functions, such as synapse formation and muscle contraction. Thus, EF responsive 4D materials could be used to incorporate electrical signals into the 4D printed scaffolds that facilitate cell-cell interactions or provide a physiologically relevant environment.

3.1.5. Bone regeneration

Aside from the impressive progress made in the above applications, 4DP has also shown promise in repairing other tissues, such as bone tissue [69]. An early application of 3DP in tissue engineering has been bone repair. Bone tissue engineering using scaffolds has been identified as a promising strategy for treating critical-sized bone defects [108, 109]. However, due to the complexity of bone defects with irregular shapes, a customized scaffold can be difficult to fit directly into irregular defects and may result in additional surgical burdens after the implant is in place [110]. The 3D printed shape memory structures can be inserted into irregular bone defect sites at the transformation temperature (T_{trans}) of shape memory materials, making them suitable candidates for use in reconstructing irregular bone damage [111]. The ability of 4D printed bone scaffolds to be easily reconfigured for minimally invasive surgery and to perfectly fit irregularly shaped defects is a major advantage [112]. They can reshape themselves to perfectly match the defect size and geometry in the host, thanks to their shape memory properties [113].

Among the various fabrication techniques available, cryogenic 3DP offers the advantage of providing scaffolds with a hierarchically porous structure, strong mechanical capabilities, and high initial loading levels [114]. It was used to fabricate photothermally-responsive shape memory

bone scaffolds with β -tricalcium phosphate/shape memory poly (lactic acid-*co*-trimethylene carbonate) (β -TCP/P(DLLA-TMC)) nanocomposites combined with biodegradable photothermal agents (i.e. black phosphorus nanosheets (BPN)) and osteoinductive agents (i.e. osteogenic peptides which are functionally similar to bone morphogenetic protein-2 and extremely effective to stimulate osteogenic differentiation *in vitro* and new bone formation *in vivo*) [115]. NIR irradiating the scaffolds caused their temperature to rapidly increase to 45 °C, causing the scaffold to morph to match the irregular shape of the bone defect. Following this, the scaffold temperature quickly dropped to 37 °C, where it regained comparable mechanical properties to that of human cancellous bone. Through micro-CT, it was observed that shape memory BPN/OP/ β -TCP/P(DLLA-TMC) scaffolds fit well into irregular cranial bone defect cavities after their implantation in the defect sites (figure 5(A)).

To achieve swelling-induce macroscopic and heat-induce microscopic changes, You *et al* developed a dual stimulus-responsive SMP [116]. Utilizing a DLP printer, the static flat surface, static micro-pillar surface, as well as the static cell culturing surface were all fabricated (figure 5(B)). The study's results indicate that the cytoskeleton spreads continuously on dynamic surfaces. While the nuclear shape on the dynamic surface initially appeared elliptical, after the micropattern transformation, it became anisotropic. Additionally, the images demonstrated that the dynamic surface affected the mechanical cue, providing further evidence that the dynamic surface regulates cell fate. The 4D printed membrane was able to regulate multiscale structural deformation *in vivo* by combining layers of SMP and hydrogel. The SMP layer provided instant topography changes at the microscale, while the light-programmable hydrogel layer enabled macroscopic fitting of defects with complex geometries.

Recently, Wang *et al* using extrusion printing, fabricated NIR-induced photothermal-responsive shape memory scaffolds in their desired open configuration [117]. After NIR application, the elastic modulus of the scaffold is greatly reduced, which allows it to adopt a temporarily closed configuration (when external force is applied); this closed shape could then be fixed by cooling down the scaffold. As a result, the closed configuration of the structure would facilitate a rapid and minimally invasive implant. Following implantation, a second exposure to NIR allowed for a precise fit at irregular bone defects. A precise fit into irregular rat cranial defects and enhanced bone regeneration were demonstrated *in vivo*.

3.1.6. Trachea repair

The trachea, also referred to as the windpipe, is a cartilaginous tube that joins the larynx to the bronchi of the lungs [118]. In the clinical setting, long segmental

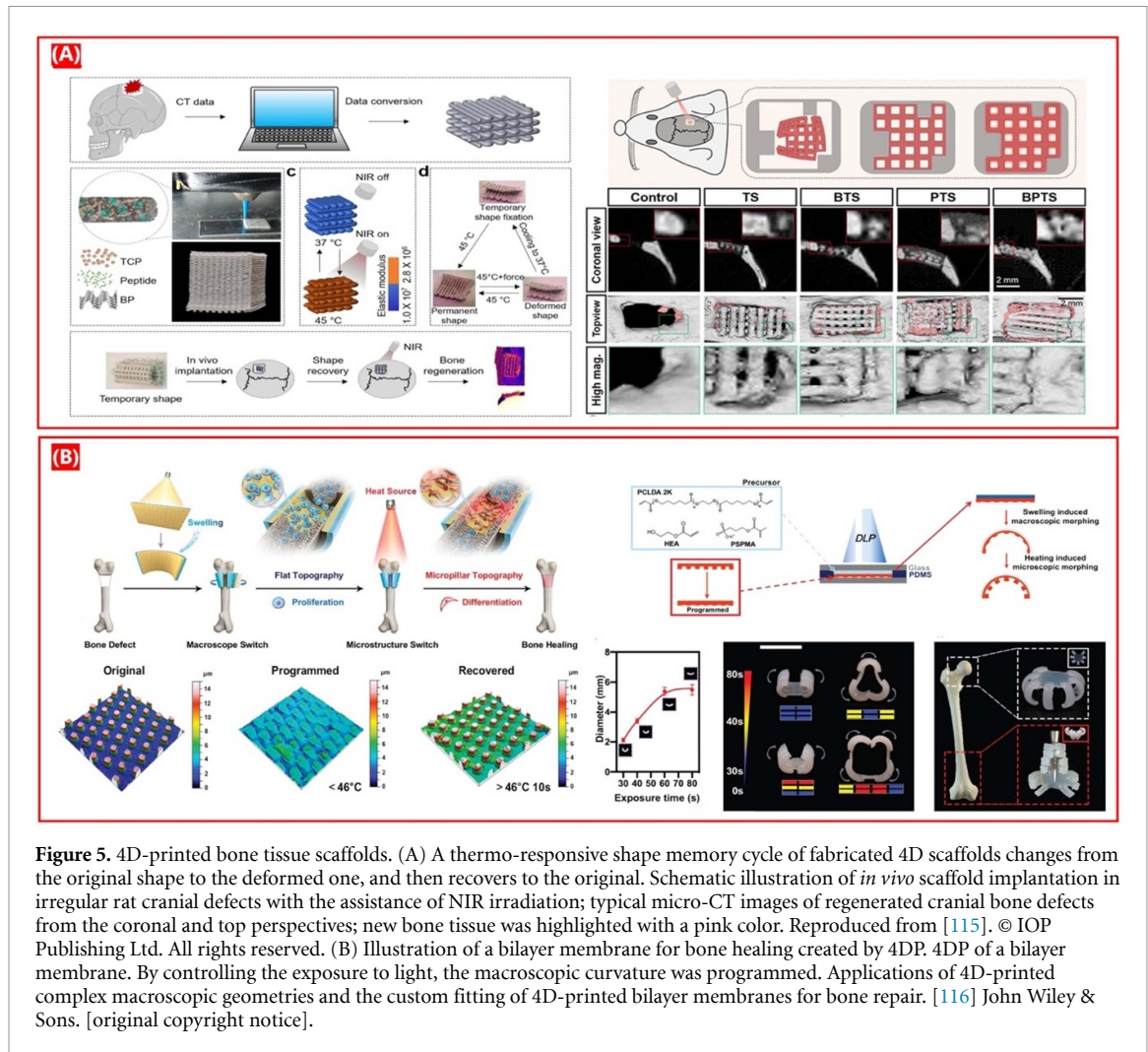


Figure 5. 4D-printed bone tissue scaffolds. (A) A thermo-responsive shape memory cycle of fabricated 4D scaffolds changes from the original shape to the deformed one, and then recovers to the original. Schematic illustration of *in vivo* scaffold implantation in irregular rat cranial defects with the assistance of NIR irradiation; typical micro-CT images of regenerated cranial bone defects from the coronal and top perspectives; new bone tissue was highlighted with a pink color. Reproduced from [115]. © IOP Publishing Ltd. All rights reserved. (B) Illustration of a bilayer membrane for bone healing created by 4DP. 4DP of a bilayer membrane. By controlling the exposure to light, the macroscopic curvature was programmed. Applications of 4D-printed complex macroscopic geometries and the custom fitting of 4D-printed bilayer membranes for bone repair. [116] John Wiley & Sons. [original copyright notice].

tracheal stenosis repair is almost impossible. To solve this unmet clinical need, tissue engineering can be used to reconstruct an artificial substitute. The development of a 4D-printed trachea with the ability to fold into C shapes is another essential application [119, 120].

Using DLP, Kim *et al* fabricated a methacrylated silk bilayer scaffold embossed with a pattern representative of tracheal rings [76]. Because the polymers were in different concentrations in each layer, the construct changed shape and self-folded as a result of differential swelling. The shape-changing behavior was better when (a) the structure was square rather than rectangular, and (b) the pattern layer was the same height as the base layer. Several cellular-laden bioinks were employed for tissue engineering applications, including adding turbinate-derived MSCs to the layer below and embedding chondrocytes in the layer above. A curvature structure was subsequently formed by immersing the scaffolds in the culture media and incubating them. Initial *in vitro* and *in vivo* studies confirmed that the 4D-bioprinted tracheal scaffolds were highly biocompatible and integrated well with the rabbit trachea.

A summary of recent applications of 4DP in the field of tissue engineering is presented in table 1. Based on the reviewed results, the 4DP has excellent potential for developing innovative biomedical tools, specifically tissue engineering.

3.2. Medical devices and soft robotics

Medical devices can be used to monitor, prevent, diagnose, prognosis, treat or mitigate illness, injury, or disability [138]. The field of medical devices has been remarkably altered by 4DP technology. Due to this, there is a growing demand for developing 4D-bioprinted dynamic implants [139]. By making dynamic biomedical implants with 4DP, it will be possible to deploy the implants in small sizes through minimally invasive surgery and then reshape the implants *in situ* to fit the defect's shape and size at the implantation sites. Integration of 4DP and soft robotics can lead to a synergistic effect in this field [140]. Soft robotics is concerned with creating soft robots capable of performing complex functions with minimal manipulation, based on the inherent elastomeric properties of soft materials [140–142]. We will discuss 4D-printed biomedical devices, stents, and soft

Table 2. Overview of 4DP applications in medical devices and soft robotics.

| Applications | Stimuli | Materials ^a | Cells | Printing techniques ^b | Reference |
|---|-----------------------------|--|-------|----------------------------------|-----------|
| Surgical suture, self-expandable stents/scaffolds | Temperature | PLMC | — | DIW | [143] |
| Suture-less sealant clips | Temperature | RS and PHBV | — | Extrusion | [144] |
| Intravascular stents | Temperature | PLA, benzophenone, and Fe ₃ O ₄ nanoparticles | — | DIW | [145] |
| Endoluminal devices | Temperature | PCL-MA | — | SLA | [72] |
| Left atrial appendage occluder | Temperature, Magnetic field | PLA and Fe ₃ O ₄ nanoparticles | — | FDM | [146] |
| Biomedical devices, soft robotics | Magnetic field | PDMS, DBP, fumed silica, and NdFeB nanoparticles | — | Extrusion | [147] |
| Wearable assistive devices | Magnetic field | Nylon and ferrofluid | — | SLS | [148] |
| Elbow protective devices | Temperature | Unsaturated PLA–PCL copolymer | — | FDM | [149] |
| Vascular repair devices | Temperature | PCL, AUD, and nBA (with/without silica nanoparticles) | — | DIW | [150] |
| Biomedical devices, soft robotics | Temperature | pAAm and pNIPAAm | — | DIW | [151] |
| Biomedical devices, soft robotics | Temperature | Alg, pNIPAAm, PEGDA, and LAPONITE® | — | Extrusion | [152] |
| Biomedical devices | Water, temperature | PU elastomer (swellable and non-swellable) and PE (heat-shrinkable) | — | Extrusion | [153] |
| On-demand microparticle capture and release | pH | Acrylic acid, pNIPAAm and PVP | — | FsLDW | [154] |
| Biomedical devices, soft robotics | Temperature, pH, enzyme | Pickering emulsion gels BSA-MA + pNIPAAm (thermo-sensitive ink), BSA-MA + p(DMAEMA) (pH-sensitive ink), BSA-MA + F127 (enzyme-sensitive ink) | — | DIW | [155] |
| Biomedical devices | Temperature | Agarose, pAAm, and LAPONITE® | — | Inkjet | [135] |
| Biomedical devices (origami-based) | Temperature | PLA | — | Extrusion | [136] |
| Soft robotics, biomedical actuators | Water | PEGDA, HEMA, SPMA, AUD, and MEO2MA | — | SLA | [137] |

^a PLMC: Poly(D,L-lactide-co-trimethylene carbonate); RS: Regenerated silk; PHBV: Poly(3-hydroxybutyrate-co-3-hydroxyvalerate); PDMS :Polydimethylsiloxane; DBP: dibutyl phthalate; NdFeB: Neodymium Iron Boron; nBA: n-butyl acrylate; PE: polyethylene, PVP: polyvinyl pyrrolidone; BSA-MA: Bovine serum albumin methacryloyl;

^b DIW: direct ink write; SLS: Selective laser sintering; FsLDW: Femtosecond laser direct writing.

robotics in this part. An overview of recent applications of 4DP in Medical devices and soft robotics is given in table 2.

3.2.1. Stents

In surgical procedures, a stent is a plastic or metal tube that maintains or restores lumen patency, wherever it is implanted (e.g. blood vessels, airways, esophagus, etc) [156–158]. There are several studies investigating the 4DP of stents in the biomedical literature. Because of the inherent capacity of 4D-printed stents

to undergo shape change, they can be deployed in a minimally invasive way at the target site in the human body to perform their roles [159, 160]. The majority of studies manipulate the shape memory effect caused by body temperature to change the shape of stents, usually between closed temporary shapes and opened ones.

Both Morrison *et al* and Zarek *et al* developed 4D-printed customizable tracheal-bronchial stents [1, 72]. When inserted into the human body, open constructs could transform from a temporarily closed

form into a permanent open one. This would allow for a minimally invasive implant and better stent fit at the damage zone. The smart stent was embedded in an infant with tracheobronchomalacia. In this way, weaning was practicable after seven days through mechanical ventilation, which was unnecessary after three weeks. However, static structures would not work in such conditions as time passed and the surrounding tissues expanded, making them unsuitable for growing infants.

Following the same strategy, Wan *et al* applied DIW to 4DP shape-morphing patient-specific flower-shaped intravascular stents using PLMC [143]. The results showed that the stents self-expanded from a closed deformed form to an expanded form when heated to 37 °C. In addition, PLMC inks could also create self-tightening surgical sutures.

Biore *et al* created a new type of thermo-responsive SMP with variable photocrosslinkable allyl groups. It was demonstrated that these SMPs were able to recover their shape and exhibited appropriate mechanical strength at body temperature [161]. A murine model of hindlimb ischemia was used to evaluate the vascular compatibility of the 4D-printed stents. Two weeks after culture, *in vivo* results revealed that the tubular structures had effectively cellularized without significant inflammatory response, did not exhibit fibrotic tissue formation, nor did they form foreign body giant cells. The results of the study suggested that SMP constructs had minimal host immune responses and good biocompatibility, which would make them an ideal material for the treatment of vascular thrombus. Furthermore, by using 4D structural elements with negative Poisson's ratios (NPRs), Wu *et al* developed self-expanding vascular stents (that could expand both radially and longitudinally under recovery temperature) [162]. Upon crimping PLA stents with NPR structures, both the radial and longitudinal dimensions decreased simultaneously. It was found that decreasing the stent diameter, increasing the wall thickness, and increasing the surface coverage could improve the radial force of PLA stents.

A similar scaffold was also developed by another research team using poly(octamethylene maleate (anhydride) citrate) [163]. The implant, which was shaped like a stent, was rolled up before injection. Then, it reabsorbed its original shape after injection, allowing engineering tissue to be implanted through a small incision. In comparison to surgically implanted scaffolds, the injected implant performed better after implantation.

In the case of narrowed or blocked branched vessels, the deployment of a bifurcated stent usually requires surgical implantation. Accordingly, Kim *et al* utilizing FDM, developed a polyurethane-based bifurcated stent inspired by Kirigami [164]. The open Y-shaped configuration changes into a temporary

closed I-shaped structure when the stent reaches its T_g (about 55 °C), where the branched tubes fold into one tube with a smaller diameter. The stent could move efficiently through the vessel while in its temporary programmed state. As a result of raised room temperatures, the vessel recovered its original Y shape after bifurcation. Thus, this advanced, 4D-printed stent can be easily implanted and can travel through the main vessel and fit appropriately into the bifurcation.

To make progress, Bodaghi *et al* constructed a tubular stent with self-expanding and shrinking characteristics [159]. Flexible SMP composite materials with T_g values around 31 °C (T_{g1}) and 64 °C (T_{g2}) were prepared for printing, by mixing two SMPs, TangoBlackPlus™ and VeroWhite-Plus™, in suitable proportions. Stents were heated to 100 °C, then axially strained and cooled at 0 °C to fixate their shape into a closed configuration, enabling easy delivery to the target site. The stents adopt an open shape to perform their supporting role upon exposure to a temperature $> T_{g1}$. An additional increase in temperature $> T_{g2}$ resulted in the recovery of the closed configuration, allowing easy removal from the target site when not required.

As a result of the improper transition temperature of SMPs, implantation becomes difficult, and there is a risk of tissue or organ frostbite or scald. Concerning this issue, Zhang and colleagues recently developed PGDA SMP with a transition temperature (T_{trans}) in the range of 20 °C–37 °C making it feasible to be conveniently programmed at room temperature and then automatically adjust to the physiological environment after being implanted into the human body [122]. A large fixity ratio of 100% at 20 °C, a significant recovery ratio of 98% at 37 °C, a cyclability of over 100 times, and a recovery speed of 0.4 s at 37 °C are the shape memory properties of these scaffolds. In addition, due to PGDA's phase transition, the Young's modulus of the scaffolds is reduced by five times, consistent with the behaviour of biological tissues. Ultimately, *in vitro* stenting and *in vivo* vascular grafting confirmed the geometrical and mechanical adaptivity of the printed structures for biomedical implantation (figure 6(A)).

Other stimuli-responsive 4D stents have been developed in addition to the thermo-responsive materials. Accordingly, a study demonstrated 4DP of both SMPs and shape memory nanocomposites (SMNCs) and prepared 4D active shape-changing structures with remotely actuated and magnetically guiding behaviours (figure 6(B)) [145]. The remote actuation of the stent system offers an effective method for designing 4D active vascular stents that can change shape and have multifunctional properties. Cabrera *et al* also proposed that a 3D-printed self-expanding polymer stent for minimally invasive heart valve regeneration using FDM technology

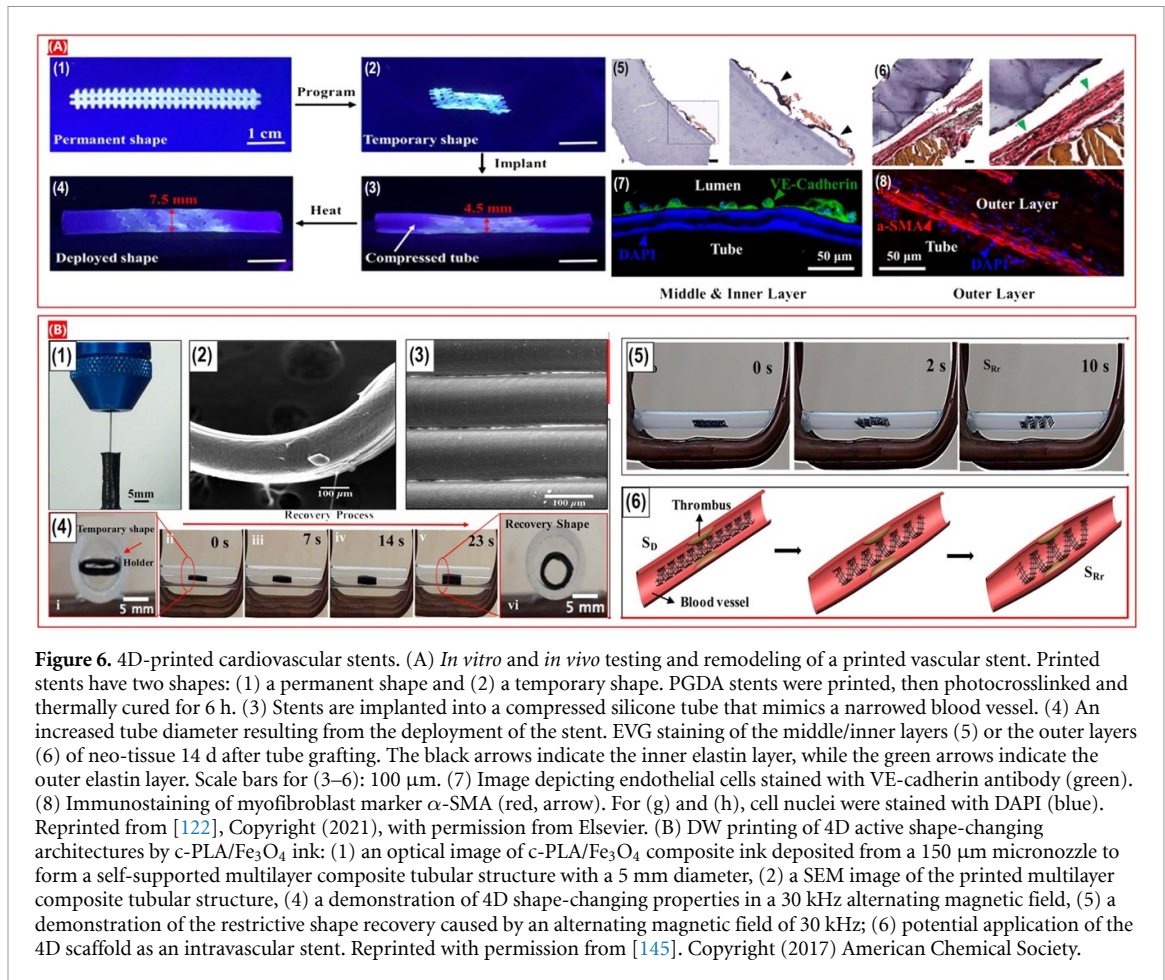


Figure 6. 4D-printed cardiovascular stents. (A) *In vitro* and *in vivo* testing and remodeling of a printed vascular stent. Printed stents have two shapes: (1) a permanent shape and (2) a temporary shape. PGDA stents were printed, then photocrosslinked and thermally cured for 6 h. (3) Stents are implanted into a compressed silicone tube that mimics a narrowed blood vessel. (4) An increased tube diameter resulting from the deployment of the stent. EVG staining of the middle/inner layers (5) or the outer layers (6) of neo-tissue 14 d after tube grafting. The black arrows indicate the inner elastin layer, while the green arrows indicate the outer elastin layer. Scale bars for (3–6): 100 μ m. (7) Image depicting endothelial cells stained with VE-cadherin antibody (green). (8) Immunostaining of myofibroblast marker α -SMA (red, arrow). For (g) and (h), cell nuclei were stained with DAPI (blue). Reprinted from [122], Copyright (2021), with permission from Elsevier. (B) DW printing of 4D active shape-changing architectures by c-PLA/Fe₃O₄ ink: (1) an optical image of c-PLA/Fe₃O₄ composite ink deposited from a 150 μ m micronozzle to form a self-supported multilayer composite tubular structure with a 5 mm diameter, (2) a SEM image of the printed multilayer composite tubular structure, (4) a demonstration of 4D shape-changing properties in a 30 kHz alternating magnetic field, (5) a demonstration of the restrictive shape recovery caused by an alternating magnetic field of 30 kHz; (6) potential application of the 4D scaffold as an intravascular stent. Reprinted with permission from [145]. Copyright (2017) American Chemical Society.

could be implanted as a similar proof-of-concept study [165]. For their stent, they used a flexible thermoplastic co-polyester elastomer, since polyesters are remarkably bioabsorbable and biodegradable polymers, mainly because their ester bonds can be hydrolyzed (as shown in figure 6(C)). Moreover, Shin *et al* constructed a shape memory tube based on an optimized microfluidic validation and computational fluid dynamics modelling approach to avoid vascular stenosis, which led to producing a successful *in vivo* stent implanted in a vessel less than 3 mm in diameter [166].

3.2.2. Other devices

Aside from stent fabrication, other smart medical devices have also been developed using 4DP technology. Through extrusion printing, Bon *et al* developed hollow cylindrical scaffolds from RS and PHBV that could act as suture-less clips for gastrointestinal anastomosis [144]. RS's negative thermal expansion coefficient is the basis of these novel structures, which result in a controlled shrinkage of the structure at 37 $^{\circ}$ C. *Ex vivo* tests showed that the porcine intestine's bursting resistance was 140% higher than that of the manually sutured intestine.

In a study presented by Zhang *et al*, 4D-printed magnetoactive soft materials (MASM) with

3D designed magnetization profiles able to adapt their shape and move were developed [147]. The researchers proposed an innovative 4DP technique that combines traditional 3D injection printing with origami-based magnetization. For the 3D injection printing of MASM, an ink was formulated with hard magnetic microparticles of neodymium magnets (NdFeB) without magnetization, PDMS, dibutyl phthalate, and fumed silica. Upon fabrication, the fabricated MASM objects were folded or bent into predesigned shapes (e.g. M-shape, U-shape, L-shape, and L-joint shape) and magnetized by an intense pulsed magnetic field (H_m). Due to its inherent elasticity, the object spontaneously transformed back into its original shape after being removed from the magnetic field. As a result, MAMS-based beams printed using 4D materials could undergo complex shape changes when a strong magnetized field is applied. Further, the authors fabricated MAMS-based robots, including a bionic human hand that played the 'rock-paper-scissors' game, as proof of concept, as shown in figure 7(A).

Lin *et al* developed another application that used the same stimulus by developing a 4D printed adsorbable left atrial appendage occluder (LAAO) [146]. By preventing LAA blood clots from reaching the bloodstream, this medical device reduces the risk

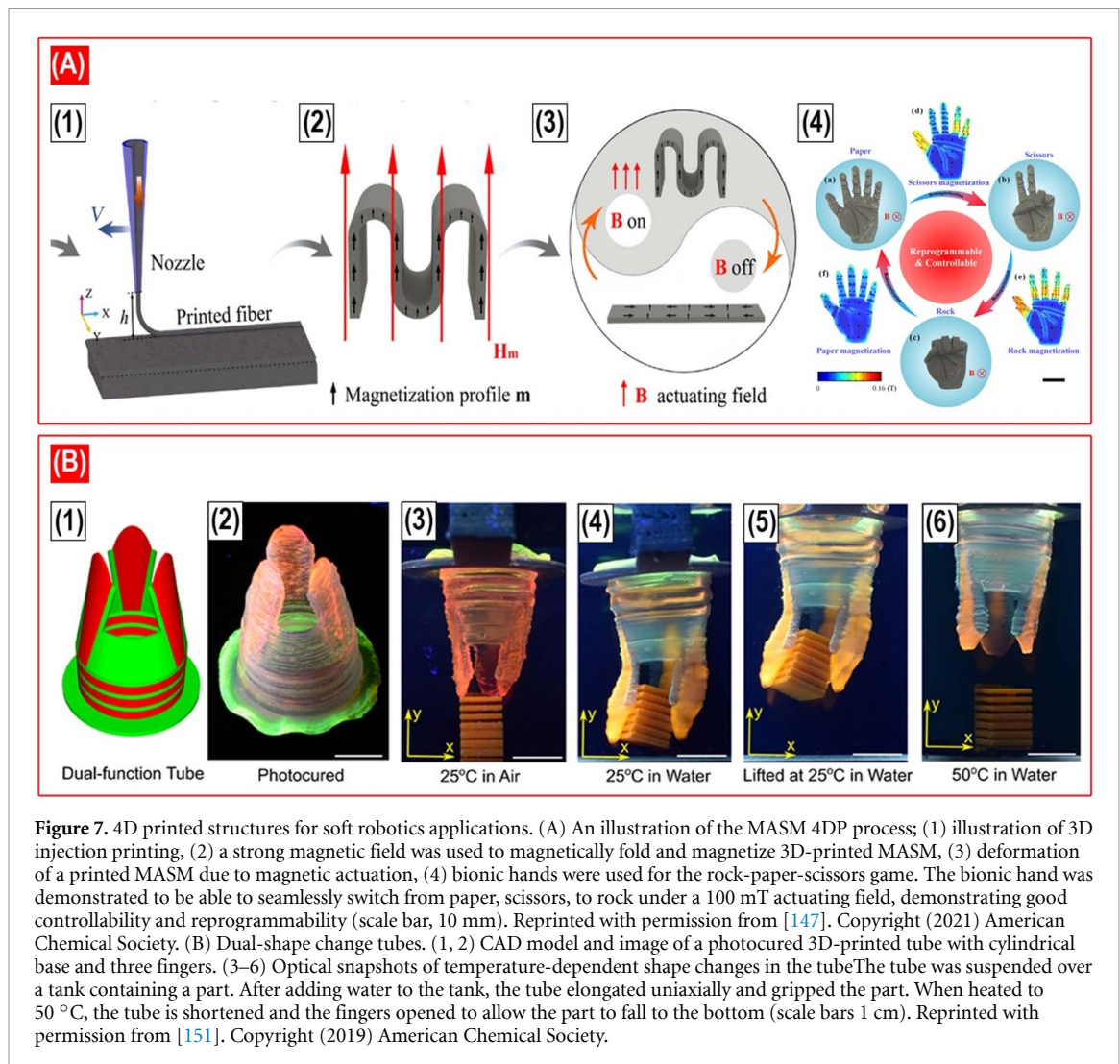


Figure 7. 4D printed structures for soft robotics applications. (A) An illustration of the MASM 4DP process; (1) illustration of 3D injection printing, (2) a strong magnetic field was used to magnetically fold and magnetize 3D-printed MASM, (3) deformation of a printed MASM due to magnetic actuation, (4) bionic hands were used for the rock-paper-scissors game. The bionic hand was demonstrated to be able to seamlessly switch from paper, scissors, to rock under a 100 mT actuating field, demonstrating good controllability and reprogrammability (scale bar, 10 mm). Reprinted with permission from [147]. Copyright (2021) American Chemical Society. (B) Dual-shape change tubes. (1, 2) CAD model and image of a photocured 3D-printed tube with cylindrical base and three fingers. (3–6) Optical snapshots of temperature-dependent shape changes in the tube. The tube was suspended over a tank containing a part. After adding water to the tank, the tube elongated uniaxially and gripped the part. When heated to 50 °C, the tube is shortened and the fingers opened to allow the part to fall to the bottom (scale bars 1 cm). Reprinted with permission from [151]. Copyright (2019) American Chemical Society.

of stroke associated with atrial fibrillation. Using FDM, the devices were generated with PLA and Fe_3O_4 magnetic nanocomposite in various geometric configurations. Further testing was conducted on the structure with the best fit to the stress–strain curve of LAA tissue. In addition to being enduring, biocompatible, and biodegradable, the device’s quick response to applied magnetic fields provided rapid control over its 4D transformation. Researchers successfully deployed LAAO in a freshly isolated swine heart to confirm the feasibility of transcatheter LAA closure.

Kuang *et al* proposed a 3D-printed complex structure (made of highly stretchable, shape-memory (SM), and self-healing (SH) elastomers) with potential application for biomedical devices, such as vascular repair devices [150]. To make tubular structures via UV-light-assisted DIW printing, they produced a semi-interpenetrating elastomer that consisted of an AUD and n-butyl acrylate photocurable resin. 600% stretchability, thermoresponsive SM property, and SM-assisted SH were demonstrated. Due to its SM properties, the tube allows for easy insertion into the

injured vessel and recovery of its initial shape after heating, enabling the tube to adhere tightly to the vessel’s inside surface.

For printing tubular geometries using DIW, Liu *et al* combined a passive, nonthermo-responsive pAAm ink material with an active, thermo-responsive pNIPAAm ink material [151]. When immersed in water at 25 °C, the objects undergo various movements (such as radial expansion, uniaxial elongation, gripping, and bending) before returning to their original shape at 50 °C. As it turns out, the type of movement depended on where the ink was placed in the tubes (figure 7(B)). A symmetric arrangement of inks either horizontally or vertically results in either linear or radial elongation. On the other hand, when inks were placed at an angle in relation to each other, tube bending was observed. The authors also developed a tubular structure with self-bending fingers that exhibits both uniaxial expansion of the central tube as well as finger gripping, a feature inspired by coral polyps. These tubes could be used for soft-robotic endoscopy and vascular implants. A more conventional application of 4D soft robots was presented

by Ilievski *et al* using 3DP and mold casting with silicone elastomers (e.g. PDMS) [167]. Soft starfish-like grippers transform into patterned channels when compressed air is applied. Because the human body has complex internal structures, micro- or nano-sized soft grippers may perform better at inaccessible sites if they maintain outstanding mobility.

3.3. Drug delivery

The term ‘drug delivery’ refers to formulations, manufacturing techniques, storage systems, and technologies that transport pharmaceutical compounds to their target sites so they can achieve the desired therapeutic effects. To enhance drug effectiveness and minimize unwanted side effects, innovative delivery systems are required as a replacement to traditional manufacturing methods characterized by a quick release. In addition, drug delivery instruments should be designed based on their specific applications to ensure their optimal performance for drug release [168–170].

The traditional healthcare model uses ‘one-size-fits-all’ criteria, which has limitations when it comes to generating accurate results due to different pharmacokinetic characteristics among patients. The variability of results associated with administering a particular drug is generally explained by differences in health background, metabolism, and genetics. Because of these differences, various patients will respond differently to prescribed medicines. It is also possible to overdose or underdose when using this traditional method [171].

There has been a growing desire to develop drugs centered on the patient in recent years. Progresses in pharmacogenetics, which can deliver more practical results, have enabled personalized medicine, which is a potential method of meeting the needs of customized medications [172]. It is likely that the future of medicine development will move away from mass production and toward a more personalized dosage approach. As a result, customized dosage can be administered to a targeted group of patients based on their metabolism homogeneity [173, 174]. The patient-centric principle may now be met with the advancement of 3DP technology. Thus, it is now possible to produce sophisticated devices that could not previously be fabricated by conventional pharmaceutical manufacturing methods [175].

Drug delivery applications for SMSs involve applications requiring both shape evolution and retention for different purposes, namely (a) maximizing the benefits of the conveyed drugs, (b) treating local diseases and (c) reducing the dosing frequency and increasing patient adherence to therapy [176–179]. Recent advancements in 4DP, i.e. 3DP of stimulus responsive materials (including SMPs), have brought further attention to using SMPs in the pharmaceutical industry due to their ability to fabricate

complex devices that shape-shift over time under the influence of an external nonmechanical stimulus [180, 181]. *In vivo* controlled drug delivery was achieved by Liu *et al* using a shape-recovering scaffold comprised of chemically crosslinked PCL [182]. Scientists incorporated growth factors into compact shape-memory porous constructs. By releasing growth factors, the scaffolds slowly regained their original shape in response to body temperature in the rabbit mandibular bone defect. Their study demonstrated that there is a high probability of implanting in dynamically altered *in vivo* environments without any meaningful impact on drug delivery (figure 8(A)).

The extended release of drugs from stomach-retained systems could be beneficial for many diseases. Gastroretentive devices can be administered in collapsed forms that are swallowed and expanded to their full size *in situ* to inhibit voidance through the wide-open pylorus. By using the shape memory properties of pharmaceutical-grade PVA, Melocchi *et al* proposed an expandable system for gastric retention [183]. Following exposure to aqueous fluids at 37 °C, a variety of original configurations were designed to facilitate gastric retention. Immediately after production, prototypes containing allopurinol were made by FDM or shaped by hot melt extruded rod templates. A variety of temporary shapes, suitable in principle for application, were created by manually deforming samples. As soon as the prototypes were submerged in 0.1 N hydrochloric solution at 37 °C, they recovered their original shape. Despite being fairly short-lived, the releases remained independent of their original shape and were significantly slowed down by the Eudragit® RS/RL-based coatings applied to the samples (figure 8(B)).

Furthermore, pH-responsive materials have been used to regulate acidification in cancerous and inflammatory areas, as well as pH differences along the digestive tract, in order to achieve controlled anti-cancer drug delivery [186, 187]. As part of Larush’s research, he designed and printed acrylic acid-based hydrogel tablets that are capable of releasing drugs at high pH [188]. Similar to Larush’s work, Okwuosa *et al* printed tablets with composite materials as the core and shell of polyvinylpyrrolidone/methacrylic acid copolymer tablets [189]. The tablets built in these two studies showed gastric resistance characteristics and pH-responsive drug release, which made them a promising method for gastrointestinal drug delivery. Through the use of enteric polymers with different grades, Goyanes and colleagues demonstrated delayed and selective release of paracetamol for tablets containing hypromellose acetate succinate. It is particularly useful for developing customized dosage medicines that can meet the needs of different patients with varying medical needs [190].

Materials responsive to magnetic fields have also been used to produce 4D-bioprinted drug delivery

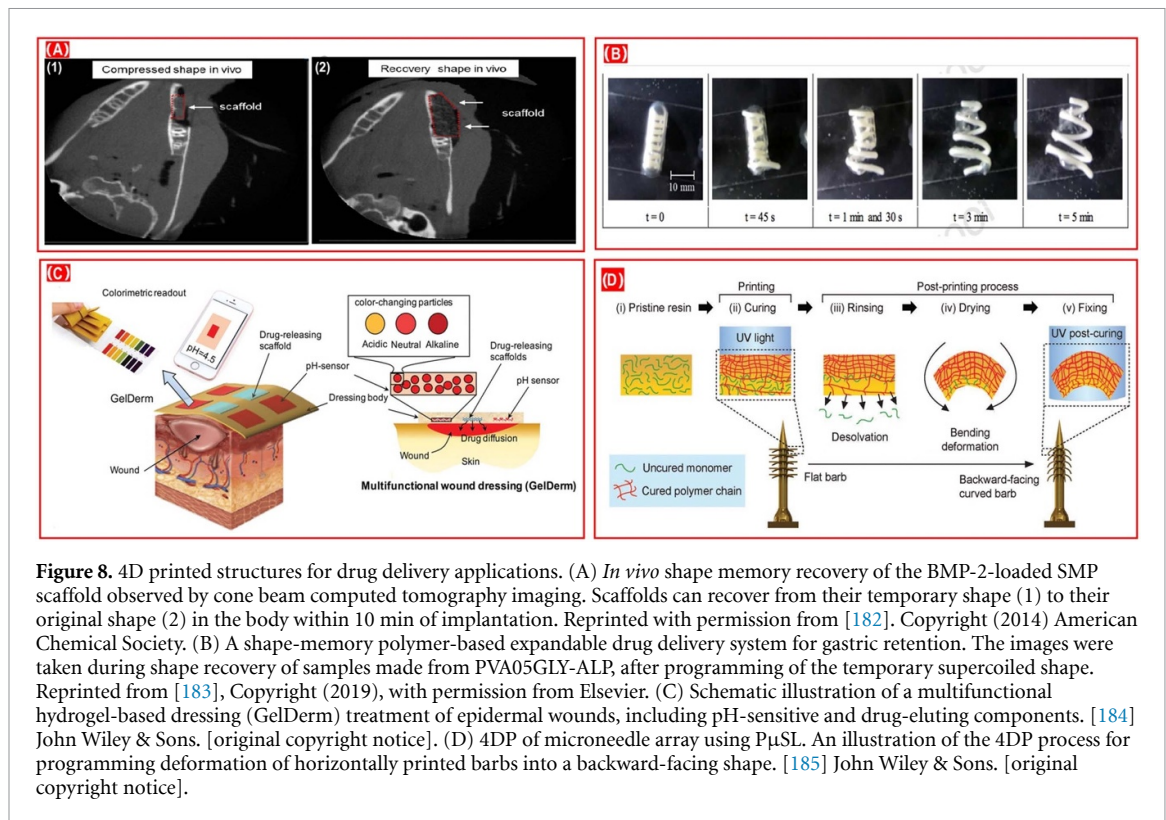


Figure 8. 4D printed structures for drug delivery applications. (A) *In vivo* shape memory recovery of the BMP-2-loaded SMP scaffold observed by cone beam computed tomography imaging. Scaffolds can recover from their temporary shape (1) to their original shape (2) in the body within 10 min of implantation. Reprinted with permission from [182]. Copyright (2014) American Chemical Society. (B) A shape-memory polymer-based expandable drug delivery system for gastric retention. The images were taken during shape recovery of samples made from PVA05GLY-ALP, after programming of the temporary supercoiled shape. Reprinted from [183], Copyright (2019), with permission from Elsevier. (C) Schematic illustration of a multifunctional hydrogel-based dressing (GelDerm) treatment of epidermal wounds, including pH-sensitive and drug-eluting components. [184] John Wiley & Sons. [original copyright notice]. (D) 4DP of microneedle array using PμSL. An illustration of the 4DP process for programming deformation of horizontally printed barbs into a backward-facing shape. [185] John Wiley & Sons. [original copyright notice].

systems [191]. To achieve the goal of building origami robots, Miyashita and colleagues printed a device that could move at a speed of 3.8 body-lengths per second in an external magnetic field [192]. In addition to its bio-resorbability and self-folding ability, this miniature untethered robotic device is also efficient at delivering drugs via heat stimulation.

It has been shown that the presence of certain enzymes such as matrix metalloproteinases (MMPs) is associated with tumour invasion and metastasis at specific sites in the body. In this way, MMP acted as a biological trigger for the release of anti-inflammatory drugs in a targeted manner from negatively charged hydrogels [193]. In this mechanism, drug-loaded hydrogels are degraded by enzymes to deliver the drugs to specific body regions as needed. Wang *et al* and Ceylan *et al* also developed micro-robots for targeting the delivery of drugs using the proteolytic degradative property of GelMA. In the presence of collagenase [194] and MMP2 enzymes [195] these magnetically driven micro-robotic devices were completely removed, leaving no detectable toxic residues behind. They have been able to tackle issues such as non-degradable or cytotoxic by-products on AM-printed micro-robots by using enzymatic degradability.

Using extrusion printing, Wang *et al* created 4D-printed patches containing alginate (Alg) and pluronic F127DA [196]. After printing, the permanent form of the patches was defined by the F127DA photocrosslinked stable network. By applying external stress to the patches, temporary folded shapes were

produced. Following this, the shapes were fixed in a calcium chloride solution bath, resulting in a second ionically crosslinked reversible calcium Alg network. Calcium ions were removed using a sodium carbonate solution, enabling permanent shape recovery in just 10 min (98.15%). Methotrexate release profiles were also evaluated. Based on the results, the surface area and shape of temporary and recovered patches have a significant impact on the drug release profiles.

As an alternative approach, 4DP technology has been used to improve drug delivery devices' tissue retentiveness rather than modify their release profiles. For example, Melocchi *et al*, used shape memory property of PVA to fabricate retentive devices with diverse geometries (U- and helix-shaped) for intravenous drug delivery systems via FDM and hot-melt extrusion [197]. The device was initially deformed by high temperatures, and it retains its original shape once exposed to water (as in the human body). They could be injected into the bladder via catheter in a temporary shape, retained in the bladder for a programmed period by recovering their original shape, and then eliminated with urine after dissolution/erosion. In addition to having the desired ability to restore the original shape, samples also showed prolonged release of a tracer, which was consistent with relevant thermo-mechanical properties. Using this 4DP approach, various drug administration channels can be developed that can be placed anywhere with minimal invasiveness and used later after they have returned to their original shape after changing shape.

Table 3. Overview of 4DP applications in drug delivery.

| Applications | Stimuli | Materials | Cells | Printing techniques | Reference |
|--|---|--|------------|---------------------|-----------|
| Drug delivery | Water, temperature | PU elastomer (swellable and non-swellable) and PE (heat-shrinkable) | — | Extrusion | [153] |
| Drug release | Magnetolectric | 4-HBA, PU-EO-PO monomer, and electro-magnetized carbon porous nanocookies | PC12 cells | DLP | [123] |
| Drug delivery system for gastric retention | Water, temperature | PVA | — | FDM | [183] |
| Drug delivery | Temperature, pH, enzyme | Pickering emulsion gels BSA-MA + pNIPAAm (thermo-sensitive ink), BSA-MA + p(DMAEMA) (pH-sensitive ink), BSA-MA + F127 (enzyme-sensitive ink) | — | DIW | [155] |
| Drug delivery (barbed microneedles) | Desolvation and drying | PEGDA | — | P μ SLA | [185] |
| Drug delivery (retentive intravesical devices) | Water | PVA and glycerol | — | FDM | [197] |
| Drug delivery (hydrogels) | Ionic crosslinking (calcium and carbonate ions) | F127DA and Alg | — | Extrusion | [196] |

In order to expedite patient care, it is paramount to detect pathogenic infections and release drugs at the wound site. A multifunctional dressing (GelDerm) was developed by Mirani *et al* that is capable of colorimetric measurement of pH, an indicator of bacterial infection, as well as release of antibiotics at the wound site (as shown in figure 8(C)). GelDerm was found to be able to detect bacteria both *in vitro* and *ex vivo*, as well as to eradicate bacteria via the sustained release of antibiotics [184].

Recently, Han *et al*, created a miniature, 4D-printed hypodermic microneedle array with backward-facing curved barbs in order to enhance tissue adhesion in the drug delivery procedure [185]. Exploiting P μ SLA, the microneedle array consisting of PEGDA was generated. Additional to this, the original constructs had barbs oriented horizontally and a gradient of crosslinking density in the photocurable polymer, i.e. the top of the barbs showed greater crosslinking than the bottom. The uncured monomers were thus desolvated when immersed in ethanol post-printing, leading to barb shrinkage and backward-facing after the drying process. One interesting finding was that this innovative microneedle array adhered 18 times better than microneedles without barbed tips. Furthermore, *ex vivo* studies using the chicken breast skin-barrier model showed prolonged drug release from microneedles (figure 8(D)). Several recent applications of 4DP in drug delivery are summarized in table 3.

4. Current limitations and future outlook

During the past several years, the field of 4DP has experienced rapid and significant advancement, especially for biomedical applications. Even so, 4DP technologies are only at the beginning of what they can achieve. While 4D bioprinting has proven capable of fabricating tissue-like structures, there are still several limitations that must be overcome. Dynamically engineered tissues, soft robotics, and implantable controlled drug delivery systems for minimally invasive surgery or patient-specific delivery encounter some challenges. Furthermore, there are a variety of concerns with this novel technique that must be addressed.

In the current state, the major challenge areas can be divided into design limitations and manufacturing limitations. Biological systems are complex, and their feedback mechanisms are complex, resulting in design-based limitations. Engineered tissues and drug delivery systems can experience problems because of oversimplification. In addition, another design limitation is the unpredictability of stimuli-driven responses of SMMs and their response times to those stimuli. A further issue that must be addressed in the near future in order to achieve the ultimate goal of 4DP research will be the activation/deactivation of 4D-printed constructs, biocompatibility, amplitude, duration, and elimination of stimuli. It may be possible to gain valuable insight into energy

transfer through materials based on computational predictions, as well as their behavior during morphing [198]. The non-linear locomotion characteristics of linear rigid materials can make these predictions very useful; however, for soft stimuli-responsive materials it can prove impossible to verify their behaviour [199]. But soon, the accumulation of experimental data and the outcome of these predictions will provide a significant database for the development of artificial intelligence systems for developing new smart materials.

In terms of manufacturing, 4DP is limited to a few 3DP technologies as well as biocompatible smart materials. Although it is cost-effective and allows printing of multiple materials, extrusion-based 4DP has significant limitations in terms of speed and resolution compared to light-assisted printing. On the other hand, light-assisted printing technologies may offer faster print speeds and higher print resolutions, but they are also expensive and do not support multiple materials.

From a material perspective, smart materials should be biocompatible and noncytotoxic as the bioprinting method relies on viable cells. In addition, nontoxic crosslinkers should be applied when stabilizing bioprinted structures. Bio-constructs that incorporate cells need to be able to crosslink properly without releasing toxic substances. Moreover, the shape-changing properties of the printed constructs should not be altered by the addition of cells or tissue [200]. To achieve both high cell viability and printability simultaneously, rheological properties must also be appropriate. As outlined above, the materials used for 4D bioprinting lack some of the desired characteristics. To solve these problems, the use of biomaterials in hybrid structures must be optimized. Additionally, the bio-printed structures should incorporate multiple smart materials to be able to respond to multiple stimuli *in vivo*. In order to deposit multi-materials precisely, high-resolution printing is needed. For precise shape morphing, precise stimulation mechanisms are also needed. A high-resolution multi-material bioprinter as well as precise stimulation methods will be needed to replicate natural tissues or organs.

Due to the fact that this advanced technique is still in its infancy, the number of smart materials applicable to biomedical applications is still limited. Currently, hydrogels and SMPs are the most common materials available for 4D bioprinting in the biomedical area. In fact, most of these materials will only respond to one stimulus, and 4D-printed constructs can only change shape in simple ways like folding, bending, curling, or flower openings and closings. This does not reflect the complex human body environment and therefore limits their potential applications in biomedicine. A major effort needs to be undertaken to develop novel stimulus-responsive shape-changing materials, not only polymers and

hydrogels, but also metals, ceramics, and composites/hybrids.

Hence, materially speaking, the introduction of novel materials/combinations of materials is needed. In this context, engineered living materials (ELMs) have the potential to meet the need for biocompatible and stimuli-responsive materials to support 4DP processes [201–203]. In the development of ELMs, bioengineered cells are used to produce materials with functionality similar to that of natural biomaterials [201]. Furthermore, these new generation materials can respond with controllable sensitivity to a variety of biosignals under a wide range of physiological conditions, making them particularly appealing for a range of biomedical applications. Despite their significant potential for 4DP, however, ELMs are concerned about scalability and high costs [201, 204, 205]. It is a relatively new technology, but 4DP has already proven its worth in the biomedical sector. With the development of affordable, high-resolution printers and the development of biologically compatible smart materials, 4DP is likely to reach its zenith soon, given its fast and sustained growth.

The bottom line is that simultaneous research and breakthroughs in 3D and 4DP will enable new technological avenues for drug delivery and pharmaceutical applications.

Data availability statement

All data that support the findings of this study are included within the article (and any supplementary files).

ORCID iDs

Moqaddaseh Afzali Naniz  <https://orcid.org/0000-0002-9807-9882>

Mohsen Askari  <https://orcid.org/0000-0002-1123-3163>

Ali Zolfagharian  <https://orcid.org/0000-0001-5302-360X>

Mehrdad Afzali Naniz  <https://orcid.org/0000-0001-9373-6276>

Mahdi Bodaghi  <https://orcid.org/0000-0002-0707-944X>

References

- [1] Morrison R J, Hollister S J, Niedner M F, Mahani M G, Park A H, Mehta D K, Ohye R G and Green G E 2015 Mitigation of tracheobronchomalacia with 3D-printed personalized medical devices in pediatric patients *Sci. Trans. Med.* **7** 285ra64
- [2] Park S A, Lee S J, Lim K S, Bae I H, Lee J H, Kim W D, Jeong M H and Park J-K 2015 *In vivo* evaluation and characterization of a bio-absorbable drug-coated stent fabricated using a 3D-printing system *Mater. Lett.* **141** 355–8
- [3] Agarwal T, Tan S-A, Onesto V, Law J X, Agrawal G, Pal S, Lim W L, Sharifi E, Moghaddam F D and Maiti T K 2021

- Engineered herbal scaffolds for tissue repair and regeneration: recent trends and technologies *Biomed. Eng. Adv.* **2** 100015
- [4] Li J, Chen M, Fan X and Zhou H 2016 Recent advances in bioprinting techniques: approaches, applications and future prospects *J. Transl. Med.* **14** 271
- [5] Agarwal T et al 2021 Recent advances in bioprinting technologies for engineering different cartilage-based tissues *Mater. Sci. Eng. C* **123** 112005
- [6] Okolie O, Stachurek I, Kandasubramanian B and Njuguna J 2020 3D printing for hip implant applications: a review *Polymers* **12** 1–29
- [7] Genova T, Roato I, Carossa M, Motta C, Cavagnetto D and Mussano F 2020 Advances on bone substitutes through 3D bioprinting *Int. J. Mol. Sci.* **21** 1–28
- [8] Javaid M and Haleem A 2020 Significant advancements of 4D printing in the field of orthopaedics *J. Clin. Orthop. Trauma* **11** S485–90
- [9] Manero A, Smith P, Sparkman J, Dombrowski M, Courbin D, Kester A, Womack I and Chi A 2019 Implementation of 3D printing technology in the field of prosthetics: past, present, and future *Int. J. Environ. Res. Public Health* **16** 1641
- [10] Park G-S, Kim S-K, Heo S-J, Koak J-Y and Seo D-G 2019 Effects of printing parameters on the fit of implant-supported 3D printing resin prosthetics *Materials* **12** 2533
- [11] Lee Ventola C 2014 Medical applications for 3D printing: current and projected uses *Pharm. Ther.* **39** 704–11
- [12] Topuz M, Dikici B, Gavgali M and Yilmazer H 2018 A review on the hydrogels used in 3D bio-printing *Int. J. 3D Print. Technol. Digit. Ind.* **2** 68–75
- [13] Liu J J, He J, Liu J J, Ma X, Chen Q, Lawrence N, Zhu W, Xu Y and Chen S 2019 Rapid 3D bioprinting of *in vitro* cardiac tissue models using human embryonic stem cell-derived cardiomyocytes *Bioprinting* **13** 1–15
- [14] Shapira A, Noor N, Oved H and Dvir T 2020 Transparent support media for high resolution 3D printing of volumetric cell-containing ECM structures *Biomed. Mater.* **15** 045018
- [15] Ng W L, Lee J M, Yeong W Y and Win Naing M 2017 Microvalve-based bioprinting-process, bio-inks and applications *Biomater. Sci.* **5** 632–47
- [16] Murphy S V S V and Atala A 2014 3D bioprinting of tissues and organs *Nat. Biotechnol.* **32** 773–85
- [17] Lu L, Mende M, Yang X, Körber H-F, Schnittler H-J, Weinert S, Heubach J, Werner C and Ravens U 2013 Design and validation of a bioreactor for simulating the cardiac niche: a system incorporating cyclic stretch, electrical stimulation, and constant perfusion *Tissue Eng. A* **19** 403–14
- [18] Gungor-Ozkerim P S, Inci I, Zhang Y S, Khademhosseini A and Dokmeci M R 2018 Bioinks for 3D bioprinting: an overview *Biomater. Sci.* **6** 915–46
- [19] Tamay D G, Usal T D, Alagoz A S, Yucel D, Hasirci N and Hasirci V 2019 3D and 4D printing of polymers for tissue engineering applications *Front. Bioeng. Biotechnol.* **7** 164
- [20] Gao B, Yang Q, Zhao X, Jin G, Ma Y and Xu F 2016 4D bioprinting for biomedical applications *Trends Biotechnol.* **34** 746–56
- [21] Kuang X, Roach D J, Wu J, Hamel C M, Ding Z, Wang T, Dunn M L and Qi H J 2019 Advances in 4D printing: materials and applications *Adv. Funct. Mater.* **29** 1805290
- [22] Polley C, Distler T, Rüffer D, Detsch R, Boccaccini A R and Seitz H 2019 3D printing of smart materials for bone regeneration *Trans. Addit. Manuf. Meets Med.* **1** S07T03
- [23] Wu J J, Huang L M, Zhao Q and Xie T 2018 4D printing: history and recent progress *Chin. J. Polym. Sci. (Engl. Ed.)* **36** 563–75
- [24] Chalissery D, Schönfeld D, Walter M, Shklyar I, Andrae H, Schwörer C, Amann T, Weisheit L and Pretsch T 2022 Highly shrinkable objects as obtained from 4D printing *Macromol. Mater. Eng.* **307** 2100619
- [25] Ionov L 2013 Biomimetic hydrogel-based actuating systems *Adv. Funct. Mater.* **23** 4555–70
- [26] Inverardi N, Pandini S, Bignotti F, Scalet G, Marconi S and Auricchio F 2020 Sequential motion of 4D printed photopolymers with broad glass transition *Macromol. Mater. Eng.* **305** 1900370
- [27] Ong C S, Nam L, Ong K, Krishnan A, Huang C Y, Fukunishi T and Hibino N 2018 3D and 4D bioprinting of the myocardium: current approaches, challenges, and future prospects *Biomed. Res. Int.* **2018** 1–11
- [28] An J, Chua C K and Mironov V 2016 A perspective on 4D bioprinting *Int. J. Bioprinting* **2** 02003
- [29] Khoo Z X, Teoh J E M, Liu Y, Chua C K, Yang S, An J, Leong K F and Yeong W Y 2015 3D printing of smart materials: a review on recent progresses in 4D printing *Virtual Phys. Prototyp.* **10** 103–22
- [30] Khalid M Y, Arif Z U and Ahmed W 2022 Four-dimensional (4D) printing: technological and manufacturing renaissance *Macromol. Mater. Eng.* **307** 2200003
- [31] Choi J, Kwon O C, Jo W, Lee H J and Moon M W 2015 4D printing technology: a review *3D Print. Addit. Manuf.* **2** 159–67
- [32] Miao S et al 2017 4D printing of polymeric materials for tissue and organ regeneration *Mater. Today* **20** 577–91
- [33] Champeau M, Heinze D A, Viana T N, de Souza E R, Chinellato A C and Titotto S 2020 4D printing of hydrogels: a review *Adv. Funct. Mater.* **30** 1910606
- [34] Zhao Q, Qi H J and Xie T 2015 Recent progress in shape memory polymer: new behavior, enabling materials, and mechanistic understanding *Prog. Polym. Sci.* **49–50** 79–120
- [35] Leist S K and Zhou J 2016 Current status of 4D printing technology and the potential of light-reactive smart materials as 4D printable materials *Virtual Phys. Prototyp.* **11** 249–62
- [36] Sydney Gladman A, Matsumoto E A, Nuzzo R G, Mahadevan L and Lewis J A 2016 Biomimetic 4D printing *Nat. Mater.* **15** 413–8
- [37] Bajpai A, Baigent A, Raghav S, Brádaigh C, Koutsos V and Radacsi N 2020 4D printing: materials, technologies, and future applications in the biomedical field *Sustainability* **12** 10628
- [38] Stroganov V, Pant J, Stoychev G, Janke A, Jehnichen D, Fery A, Handa H and Ionov L 2018 4D biofabrication: 3D cell patterning using shape-changing films *Adv. Funct. Mater.* **28** 1706248
- [39] Bakarich S E, Gorkin R III, Panhuis M and Spinks G M 2015 4D printing with mechanically robust, thermally actuating hydrogels *Macromol. Rapid Commun.* **36** 1211–7
- [40] Yang G H, Yeo M, Koo Y W and Kim G H 2019 4D bioprinting: technological advances in biofabrication *Macromol. Biosci.* **19** 1800441
- [41] Suntornnond R, An J and Chua C K 2017 Bioprinting of thermoresponsive hydrogels for next generation tissue engineering: a review *Macromol. Mater. Eng.* **302** 1600266
- [42] Taylor J M, Luan H, Lewis J A, Rogers J A, Nuzzo R G and Braun P V 2022 Biomimetic and biologically compliant soft architectures via 3D and 4D assembly methods: a perspective *Adv. Mater.* **34** 2108391
- [43] Ali M H, Abilgazyev A and Adair D 2019 4D printing: a critical review of current developments, and future prospects *Int. J. Adv. Manuf. Technol.* **105** 701–17
- [44] Haleem A, Javaid M, Singh R P and Suman R 2021 Significant roles of 4D printing using smart materials in the field of manufacturing *Adv. Ind. Eng. Polym. Res.* **4** 301–11
- [45] Patil A N and Sarje S H 2021 Additive manufacturing with shape changing/memory materials: a review on 4D printing technology *Mater. Today: Proc.* **44** 1744–9
- [46] Han M, Yang Y and Li L 2022 Techno-economic modeling of 4D printing with thermo-responsive materials towards desired shape memory performance *IISE Trans.* **54** 1047–59
- [47] Feng R, Xu Y, Han H, Huang W, Wang Y and Li X 2021 Printing method, driving mechanism, deformation mode

- and application of 4D printing shape memory polymers *Mater. Rep.* **35** 5147–57
- [48] Joshi S, Rawat K, C K, Rajamohan V, Mathew A T, Koziol K, Kumar Thakur V and Balan A S S 2020 4D printing of materials for the future: opportunities and challenges *Appl. Mater. Today* **18** 100490
- [49] Yarali E et al 2022 Magneto-/electro-responsive polymers toward manufacturing, characterization, and biomedical/soft robotic applications *Appl. Mater. Today* **26** 101306
- [50] Goudu S R, Yasa I C, Hu X, Ceylan H, Hu W and Sitti M 2020 Biodegradable untethered magnetic hydrogel Milli-Grippers *Adv. Funct. Mater.* **30** 2004975
- [51] Zhang Z, Demir K G and Gu G X 2019 Developments in 4D-printing: a review on current smart materials, technologies, and applications *Int. J. Smart Nano Mater.* **10** 205–24
- [52] Mallakpour S, Tabesh F and Hussain C M 2021 3D and 4D printing: from innovation to evolution *Adv. Colloid Interface Sci.* **294** 102482
- [53] Muzaffar A, Ahamed M B, Deshmukh K, Kovářik T, Křenek T and Pasha S K K 2020 3D and 4D printing of pH-responsive and functional polymers and their composites *3D and 4D Printing of Polymer Nanocomposite Materials: Processes, Applications, and Challenges* (Amsterdam, Netherlands: Elsevier) (<https://doi.org/10.1016/B978-0-12-816805-9.00004-1>)
- [54] Zeng Y, Jiang L, He Q, Wodnicki R, Yang Y, Chen Y and Zhou Q 2022 Recent progress in 3D printing piezoelectric materials for biomedical applications *J. Phys. D: Appl. Phys.* **55** 013002
- [55] Sahafnejad-Mohammadi I, Karamimoghdam M, Zolfagharian A, Akrami M and Bodaghi M 2022 4D printing technology in medical engineering: a narrative review *J. Brazilian Soc. Mech. Sci. Eng.* **44** 233
- [56] Bodaghi M, Damanpack A R and Liao W H 2017 Adaptive metamaterials by functionally graded 4D printing *Mater. Des.* **135** 26–36
- [57] Yang C, Tian X, Liu T, Cao Y and Li D 2017 3D printing for continuous fiber reinforced thermoplastic composites: mechanism and performance *Rapid Prototyp. J.* **23** 209–15
- [58] Ahmed A, Arya S, Gupta V, Furukawa H and Khosla A 2021 4D printing: fundamentals, materials, applications and challenges *Polymer* **228** 123926
- [59] Clark E A, Alexander M R, Irvine D J, Roberts C J, Wallace M J, Sharpe S, Yoo J, Hague R J M, Tuck C J and Wildman R D 2017 3D printing of tablets using inkjet with UV photoinitiation *Int. J. Pharm.* **529** 523–30
- [60] Murthy H, Thakur N and Shankwar N 2020 Nickel-based inks for flexible electronics—a review on recent trends *J. Adv. Manuf. Syst.* **1**–34
- [61] Quan H, Zhang T, Xu H, Luo S, Nie J and Zhu X 2020 Photo-curing 3D printing technique and its challenges *Bioact. Mater.* **5** 110–5
- [62] Mitchell A, Lafont U, Holyńska M and Semprimoschnig C 2018 Additive manufacturing—a review of 4D printing and future applications *Addit. Manuf.* **24** 606–26
- [63] Zhou L-Y, Fu J and He Y 2020 A review of 3D printing technologies for soft polymer materials *Adv. Funct. Mater.* **30** 2000187
- [64] Yu C, Schimelman J, Wang P, Miller K L, Ma X, You S, Guan J, Sun B, Zhu W and Chen S 2020 Photopolymerizable biomaterials and light-based 3D printing strategies for biomedical applications *Chem. Rev.* **120** 10695–743
- [65] Khademhosseini A and Langer R 2016 A decade of progress in tissue engineering *Nat. Protocols* **11** 1775–81
- [66] Saska S, Pilatti L, Blay A and Shibli J A 2021 Bioresorbable polymers: advanced materials and 4D printing for tissue engineering *Polymers* **13** 563
- [67] Agarwal T, Subramanian B and Maiti T K 2019 Liver tissue engineering: challenges and opportunities *ACS Biomater. Sci. Eng.* **5** 4167–82
- [68] Karageorgiou V and Kaplan D 2005 Porosity of 3D biomaterial scaffolds and osteogenesis *Biomaterials* **26** 5474–91
- [69] Yang Q, Gao B and Xu F 2020 Recent advances in 4D bioprinting *Biotechnol. J.* **15** 1900086
- [70] Wang Y, Cui H, Esworthy T, Mei D, Wang Y and Zhang L G 2021 Emerging 4D printing strategies for next-generation tissue regeneration and medical devices *Adv. Mater.* **34** 2109198
- [71] Wang C, Zhou Y and Wang M 2017 *In situ* delivery of rhBMP-2 in surface porous shape memory scaffolds developed through cryogenic 3D plotting *Mater. Lett.* **189** 140–3
- [72] Zarek M, Mansour N, Shapira S and Cohn D 2017 4D printing of shape memory-based personalized endoluminal medical devices *Macromol. Rapid Commun.* **38** 1600628
- [73] Miao S, Zhu W, Castro N J, Nowicki M, Zhou X, Cui H, Fisher J P and Zhang L G 2016 4D printing smart biomedical scaffolds with novel soybean oil epoxidized acrylate *Sci. Rep.* **6** 27226
- [74] Hendrikson W J, Rouwkema J, Clementi F, van Blitterswijk C A, Farè S and Moroni L 2017 Towards 4D printed scaffolds for tissue engineering: exploiting 3D shape memory polymers to deliver time-controlled stimulus on cultured cells *Biofabrication* **9** 031001
- [75] Kirillova A, Maxson R, Stoychev G, Gomillion C T and Ionov L 2017 4D biofabrication using shape-morphing hydrogels *Adv. Mater.* **29** 1703443
- [76] Kim S H et al 2020 4D-bioprinted silk hydrogels for tissue engineering *Biomaterials* **260** 120281
- [77] Luo Y, Lin X, Chen B and Wei X 2019 Cell-laden four-dimensional bioprinting using near-infrared-triggered shape-morphing alginate/polydopamine bioinks *Biofabrication* **11** 045019
- [78] Brassard J A, Nikolaev M, Hübscher T, Hofer M and Lutolf M P 2021 Recapitulating macro-scale tissue self-organization through organoid bioprinting *Nat. Mater.* **20** 22–29
- [79] Goulart E et al 2020 3D bioprinting of liver spheroids derived from human induced pluripotent stem cells sustain liver function and viability *in vitro* *Biofabrication* **12** 015010
- [80] Skylar-Scott M A, Uzel S G M, Nam L L, Ahrens J H, Truby R L, Damaraju S and Lewis J A 2019 Biomanufacturing of organ-specific tissues with high cellular density and embedded vascular channels *Sci. Adv.* **5** eaaw2459
- [81] Kuribayashi-Shigetomi K, Onoe H, Takeuchi S and Han A 2012 Cell origami: self-folding of three-dimensional cell-laden microstructures driven by cell traction force *PLoS One* **7** e51085
- [82] Patel D K, Sakhaei A H, Layani M, Zhang B, Ge Q and Magdassi S 2017 Highly stretchable and UV curable elastomers for digital light processing based 3D printing *Adv. Mater.* **29** 1606000
- [83] Jamal M, Kadam S S, Xiao R, Jivan F, Onn T-M, Fernandes R, Nguyen T D and Gracias D H 2013 Bio-origami hydrogel scaffolds composed of photocrosslinked PEG bilayers *Adv. Healthcare Mater.* **2** 1142–50
- [84] Zhang L et al 2020 A biomimetic 3D-self-forming approach for microvascular scaffolds *Adv. Sci.* **7** 1903553
- [85] Lai J, Li J and Wang M 2020 3D printed porous tissue engineering scaffolds with the self-folding ability and controlled release of growth factor *MRS Commun.* **10** 579–86
- [86] Cui C, Kim D-O, Pack M Y, Han B, Han L, Sun Y and Han L-H 2020 4D printing of self-folding and cell-encapsulating 3D microstructures as scaffolds for tissue-engineering applications *Biofabrication* **12** 045018
- [87] Constante G, Apsite I, Alkhamis H, Dulle M, Schwarzer M, Caspari A, Synytska A, Salehi S and Ionov L 2021 4D biofabrication using a combination of 3D printing and

- melt-electrowriting of shape-morphing polymers *ACS Appl. Mater. Interfaces* **13** 12767–76
- [88] Budharaju H, Subramanian A and Sethuraman S 2021 Recent advancements in cardiovascular bioprinting and bioprinted cardiac constructs *Biomater. Sci.* **9** 1974–94
- [89] Hong S, Kim J S, Jung B, Won C and Hwang C 2019 Coaxial bioprinting of cell-laden vascular constructs using a gelatin-tyramine bioink *Biomater. Sci.* **7** 4578–87
- [90] Azhar Z, Haque N, Ali S, Mozafari M and Sefat F 2019 Bioengineered cardiac patch scaffolds *Handbook of Tissue Engineering Scaffolds* vol 1 (Cambridge: Woodhead Publishing) pp 705–28
- [91] Askari M, Afzali Naniz M, Kouhi M, Saberi A, Zolfagharian A and Bodaghi M 2021 Recent progress in extrusion 3D bioprinting of hydrogel biomaterials for tissue regeneration: a comprehensive review with focus on advanced fabrication techniques *Biomater. Sci.* **9** 535–73
- [92] Miao S *et al* 2018 Photolithographic-stereolithographic-tandem fabrication of 4D smart scaffolds for improved stem cell cardiomyogenic differentiation *Biofabrication* **10** 035007
- [93] Wang Y, Cui H, Wang Y, Xu C, Esworthy T J, Hann S Y, Boehm M, Shen Y L, Mei D and Zhang L G 2021 4D printed cardiac construct with aligned myofibers and adjustable curvature for myocardial regeneration *ACS Appl. Mater. Interfaces* **13** 12746–58
- [94] Cui H *et al* 2020 4D physiologically adaptable cardiac patch: a 4-month *in vivo* study for the treatment of myocardial infarction *Sci. Adv.* **6** eabb5067
- [95] Cui H, Miao S, Esworthy T, Lee S-J, Zhou X, Hann S Y, Webster T J, Harris B T and Zhang L G 2019 A novel near-infrared light responsive 4D printed nanoarchitecture with dynamically and remotely controllable transformation *Nano Res.* **12** 1381–8
- [96] Ma S Q, Zhang Y P, Wang M, Liang Y H, Ren L and Ren L Q 2020 Recent progress in 4D printing of stimuli-responsive polymeric materials *Sci. China Technol. Sci.* **63** 532–44
- [97] Huang G, Li F, Zhao X, Ma Y, Li Y, Lin M, Jin G, Lu T J, Genin G M and Xu F 2017 Functional and biomimetic materials for engineering of the three-dimensional cell microenvironment *Chem. Rev.* **117** 12764–850
- [98] Hegde S and Hsiao A 2016 Improving the Fontan: pre-surgical planning using four dimensional (4D) flow, bio-mechanical modeling and three dimensional (3D) printing *Prog. Pediatr. Cardiol.* **43** 57–60
- [99] Lee S-J, Esworthy T, Stake S, Miao S, Zuo Y Y, Harris B T and Zhang L G 2018 Advances in 3D bioprinting for neural tissue engineering *Adv. Biosyst.* **2** 1700213
- [100] Yoo J *et al* 2020 Augmented peripheral nerve regeneration through elastic nerve guidance conduits prepared using a porous PLCL membrane with a 3D printed collagen hydrogel *Biomater. Sci.* **8** 6261–71
- [101] Miao S, Cui H, Nowicki M, Xia L, Zhou X, Lee S-J, Zhu W, Sarkar K, Zhang Z and Zhang L G 2018 Stereolithographic 4D bioprinting of multiresponsive architectures for neural engineering *Adv. Biosyst.* **2** 1800101
- [102] Miao S, Cui H, Esworthy T, Mahadik B, Lee S J, Zhou X, Hann S Y, Fisher J P and Zhang L G 2020 4D self-morphing culture substrate for modulating cell differentiation *Adv. Sci.* **7** 1902403
- [103] Stewart G 2009 *The Skeletal And Muscular Systems* (New York: Chelsea House) pp 10–14
- [104] Ostrovidov S, Hosseini V, Ahadian S, Fujie T, Parthiban S P, Ramalingam M, Bae H, Kaji H and Khademhosseini A 2014 Skeletal muscle tissue engineering: methods to form skeletal myotubes and their applications *Tissue Eng. B* **20** 403–36
- [105] Seyedmahmoud S, Celebi-Saltik Ç-S, Barros B, Nasiri N, Banton B, Shamloo S, Ashammakhi A, Dokmeci D and Ahadian A 2019 Three-dimensional bioprinting of functional skeletal muscle tissue using gelatin methacryloyl-alginate bioinks *Micromachines* **10** 679
- [106] Li X, Wang X, Chen H, Jin Z, Dai X, Zhang X, Zhang L and Xu T 2019 A comparative study of the behavior of neural progenitor cells in extrusion-based *in vitro* hydrogel models *Biomed. Mater.* **14** 65001
- [107] Yang G H, Kim W, Kim J and Kim G H 2020 A skeleton muscle model using GelMA-based cell-aligned bioink processed with an electric-field assisted 3D/4D bioprinting *Theranostics* **11** 48–63
- [108] Wen Y, Xun S, Haoye M, Baichuan S, Peng C, Xuejian L, Kaihong Z, Xuan Y, Jiang P and Shibi L 2017 3D printed porous ceramic scaffolds for bone tissue engineering: a review *Biomater. Sci.* **5** 1690–8
- [109] Gupta D, Vashisth P and Bellare J 2021 Multiscale porosity in a 3D printed gellan–gelatin composite for bone tissue engineering *Biomed. Mater.* **16** 034103
- [110] Zhang D, George O J, Petersen K M, Jimenez-Vergara A C, Hahn M S and Grunlan M A 2014 A bioactive “self-fitting” shape memory polymer scaffold with potential to treat cranio-maxillo facial bone defects *Acta Biomater.* **10** 4597–605
- [111] Wang L, Qiu Y, Lv H, Si Y, Liu L, Zhang Q, Cao J, Yu J, Li X and Ding B 2019 3D superelastic scaffolds constructed from flexible inorganic nanofibers with self-fitting capability and tailorable gradient for bone regeneration *Adv. Funct. Mater.* **29** 1901407
- [112] Shakibania S, Ghazanfari L, Raeeszadeh-Sarmazdeh M and Khakbiz M 2021 Medical application of biomimetic 4D printing *Drug Dev. Ind. Pharm.* **47** 521–34
- [113] Wan Z, Zhang P, Liu Y, Lv L and Zhou Y 2020 Four-dimensional bioprinting: current developments and applications in bone tissue engineering *Acta Biomater.* **101** 26–42
- [114] Wang C, Zhao Q and Wang M 2017 Cryogenic 3D printing for producing hierarchical porous and rhBMP-2-loaded Ca-P/PLLA nanocomposite scaffolds for bone tissue engineering *Biofabrication* **9** 025031
- [115] Wang C *et al* 2020 Advanced reconfigurable scaffolds fabricated by 4D printing for treating critical-size bone defects of irregular shapes *Biofabrication* **12** 045025
- [116] You D *et al* 2021 4D printing of multi-responsive membrane for accelerated *in vivo* bone healing via remote regulation of stem cell fate *Adv. Funct. Mater.* **31** 2103920
- [117] Lai J, Wang C and Wang M 2021 3D printing in biomedical engineering: processes, materials, and applications *Appl. Phys. Rev.* **8** 021322
- [118] Ahn C B, Son K H, Yu Y S, Kim T H, Lee J I and Lee J W 2019 Development of a flexible 3D printed scaffold with a cell-adhesive surface for artificial trachea *Biomed. Mater.* **14** 055001
- [119] Greaney A M and Niklason L E 2021 The history of engineered tracheal replacements: interpreting the past and guiding the future *Tissue Eng. B* **27** 341–52
- [120] Gao M *et al* 2017 Tissue-engineered trachea from a 3D-printed scaffold enhances whole-segment tracheal repair *Sci. Rep.* **7** 5246
- [121] Yang C, Luo J, Polunas M, Bosnjak N, Chueng S-T D, Chadwick M, Sabaawy H E, Chester S A, Lee K-B and Lee H 2020 4D-printed transformable tube array for high-throughput 3D cell culture and histology *Adv. Mater.* **32** 2004285
- [122] Zhang C, Cai D, Liao P, Su J-W, Deng H, Vardhanabhuti B, Ulery B D, Chen S-Y and Lin J 2021 4D printing of shape-memory polymeric scaffolds for adaptive biomedical implantation *Acta Biomater.* **122** 101–10
- [123] Fang J-H, Hsu -H-H, Hsu R-S, Peng C-K, Lu Y-J, Chen Y-Y, Chen S-Y and Hu S-H 2020 4D printing of stretchable nanocookie@conduit material hosting biocues and magnetoelectric stimulation for neurite sprouting *NPG Asia Mater.* **12** 61
- [124] Lee Y B, Jeon O, Lee S J, Ding A, Wells D and Alsborg E 2021 Induction of four-dimensional spatiotemporal geometric transformations in high cell density tissues via shape-changing hydrogels *Adv. Funct. Mater.* **31** 2010104

- [125] Ding A, Lee S J, Ayyagari S, Tang R, Huynh C T and Alsberg E 2022 4D biofabrication via instantly generated graded hydrogel scaffolds *Bioact. Mater.* **7** 324–32
- [126] Wang Y-J, Jeng U-S and Hsu S-H 2018 Biodegradable water-based polyurethane shape memory elastomers for bone tissue engineering *ACS Biomater. Sci. Eng.* **4** 1397–406
- [127] Le Fer G and Becker M L 2020 4D printing of resorbable complex shape-memory poly(propylene fumarate) star scaffolds *ACS Appl. Mater. Interfaces* **12** 22444–52
- [128] Devillard C D, Mandon C A, Lambert S A, Blum L J and Marquette C A 2018 Bioinspired multi-activities 4D printing objects: a new approach toward complex tissue engineering *Biotechnol. J.* **13** 1800098
- [129] Miao S, Zhu W, Castro N J, Leng J and Zhang L G 2016 Four-dimensional printing hierarchy scaffolds with highly biocompatible smart polymers for tissue engineering applications *Tissue Eng. C* **22** 952–63
- [130] Zhao W, Zhang F, Leng J and Liu Y 2019 Personalized 4D printing of bioinspired tracheal scaffold concept based on magnetic stimulated shape memory composites *Compos. Sci. Technol.* **184** 107866
- [131] Miao S, Nowicki M, Cui H, Lee S-J, Zhou X, Mills D K and Zhang L G 2019 4D anisotropic skeletal muscle tissue constructs fabricated by staircase effect strategy *Biofabrication* **11** 035030
- [132] Uribe-Gomez J et al 2021 Shape-morphing fibrous hydrogel/elastomer bilayers fabricated by a combination of 3D printing and melt electrowriting for muscle tissue regeneration *ACS Appl. Bio Mater.* **4** 1720–30
- [133] Ko H, Ratri M C, Kim K, Jung Y, Tae G and Shin K 2020 Formulation of sugar/hydrogel inks for rapid thermal response 4D architectures with sugar-derived macropores *Sci. Rep.* **10** 7527
- [134] Seo J W, Shin S R, Park Y J and Bae H 2020 Hydrogel production platform with dynamic movement using photo-crosslinkable/temperature reversible chitosan polymer and stereolithography 4D printing technology *J. Tissue Eng. Regen. Med.* **17** 423–31
- [135] Guo J, Zhang R, Zhang L and Cao X 2018 4D printing of robust hydrogels consisted of agarose nanofibers and polyacrylamide *ACS Macro Lett.* **7** 442–6
- [136] Langford T, Mohammed A, Essa K, Elshaer A and Hassanin H 2021 4d printing of origami structures for minimally invasive surgeries using functional scaffold *Appl. Sci.* **11** 332
- [137] Ji Z, Yan C, Yu B, Zhang X, Cai M, Jia X, Wang X and Zhou F 2019 3D printing of hydrogel architectures with complex and controllable shape deformation *Adv. Mater. Technol.* **4** 1800713
- [138] Ahluwalia A et al 2018 Towards open source medical devices current situation, inspiring advances and challenges *BIODEVICES 2018–11th Int. Conf. on Biomedical Electronics and Devices, Proc.; Part of 11th Int. Joint Conf. on Biomedical Engineering Systems and Technologies, BIOSTEC 2018 vol 1* (<https://doi.org/10.5220/0006586501410149>)
- [139] Lai J, Ye X, Liu J, Wang C, Li J, Wang X, Ma M and Wang M 2021 4D printing of highly printable and shape morphing hydrogels composed of alginate and methylcellulose *Mater. Des.* **205** 109699
- [140] Whitesides G M 2018 Soft robotics *Angew. Chem., Int. Ed.* **57** 4258–73
- [141] Polygerinos P, Wang Z, Galloway K C, Wood R J and Walsh C J 2015 Soft robotic glove for combined assistance and at-home rehabilitation *Robot. Auton. Syst.* **73** 135–43
- [142] Zolfagharian A, Kaynak A, Bodaghi M, Kouzani A Z, Gharraie S and Nahavandi S 2020 Control-based 4D printing: adaptive 4D-printed systems *Appl. Sci.* **10** 3020
- [143] Wan X, Wei H, Zhang F, Liu Y and Leng J 2019 3D printing of shape memory poly(d,l-lactide-co-trimethylene carbonate) by direct ink writing for shape-changing structures *J. Appl. Polym. Sci.* **136** 48177
- [144] Bittolo Bon S, Chiesa I, Morselli D, Degli Esposti M, Fabbri P, De Maria C, Foggi Viligiardi T, Morabito A, Giorgi G and Valentini L 2021 Printable smart 3D architectures of regenerated silk on poly(3-hydroxybutyrate-co-3-hydroxyvalerate) *Mater. Des.* **201** 109492
- [145] Wei H, Zhang Q, Yao Y, Liu L, Liu Y and Leng J 2017 Direct-write fabrication of 4D active shape-changing structures based on a shape memory polymer and its nanocomposite *ACS Appl. Mater. Interfaces* **9** 876–83
- [146] Lin C, Liu L, Liu Y and Leng J 2021 4D printing of bioinspired absorbable left atrial appendage occluders: a proof-of-concept study *ACS Appl. Mater. Interfaces* **13** 12668–78
- [147] Zhang Y, Wang Q, Yi S, Lin Z, Wang C, Chen Z and Jiang L 2021 4D printing of magnetoactive soft materials for on-demand magnetic actuation transformation *ACS Appl. Mater. Interfaces* **13** 4174–84
- [148] Ploszajski A R, Jackson R, Ransley M and Miodownik M 2019 4D printing of magnetically functionalized chainmail for exoskeletal biomedical applications *MRS Adv.* **4** 1361–6
- [149] Cheng C-Y, Xie H, Xu Z-Y, Li L, Jiang M-N, Tang L, Yang K-K and Wang Y-Z 2020 4D printing of shape memory aliphatic copolyester via UV-assisted FDM strategy for medical protective devices *Chem. Eng. J.* **396** 125242
- [150] Kuang X, Chen K, Dunn C K, Wu J, Li V C F and Qi H J 2018 3D printing of highly stretchable, shape-memory, and self-healing elastomer toward novel 4D printing *ACS Appl. Mater. Interfaces* **10** 7381–8
- [151] Liu J et al 2019 Dual-gel 4D printing of bioinspired tubes *ACS Appl. Mater. Interfaces* **11** 8492–8
- [152] Simińska-Stanny J, Nizioł M, Szymczyk-Ziółkowska P, Brożyna M, Junka A, Shavandi A and Podstawczyk D 2022 4D printing of patterned multimaterial magnetic hydrogel actuators *Addit. Manuf.* **49** 102506
- [153] Song Z, Ren L, Zhao C, Liu H, Yu Z, Liu Q and Ren L 2020 Biomimetic nonuniform, dual-stimuli self-morphing enabled by gradient four-dimensional printing *ACS Appl. Mater. Interfaces* **12** 6351–61
- [154] Hu Y et al 2020 Botanical-inspired 4D printing of hydrogel at the microscale *Adv. Funct. Mater.* **30** 1907377
- [155] Narupai B, Smith P T and Nelson A 2021 4D printing of multi-stimuli responsive protein-based hydrogels for autonomous shape transformations *Adv. Funct. Mater.* **31** 2011012
- [156] Stoeckel D, Bonsignore C and Duda S 2002 A survey of stent designs *Minim. Invasive Ther. Allied Technol.* **11** 137–47
- [157] Kang Y 2019 A review of self-expanding esophageal stents for the palliation therapy of inoperable esophageal malignancies *Biomed. Res. Int.* **2019** 1–11
- [158] Scafa Udriște A, Niculescu A-G, Grumezescu A M and Bădilă E 2021 Cardiovascular stents: a review of past, current, and emerging devices *Materials* **14** 2498
- [159] Bodaghi M, Damanpack A R and Liao W H 2016 Self-expanding/shrinking structures by 4D printing *Smart Mater. Struct.* **25** 105034
- [160] van Manen T, Janbaz S, Jansen K M B and Zadpoor A A 2021 4D printing of reconfigurable metamaterials and devices *Commun. Mater.* **2** 56
- [161] Boire T C, Gupta M K, Zachman A L, Lee S H, Balikov D A, Kim K, Bellan L M and Sung H-J 2016 Reprint of: pendant allyl crosslinking as a tunable shape memory actuator for vascular applications *Acta Biomater.* **34** 73–83
- [162] Wu Z, Zhao J, Wu W, Wang P, Wang B, Li G and Zhang S 2018 Radial compressive property and the proof-of-concept study for realizing self-expansion of 3D printing polylactic acid vascular stents with negative poisson's ratio structure *Materials* **11** 1357
- [163] Montgomery M et al 2017 Flexible shape-memory scaffold for minimally invasive delivery of functional tissues *Nat. Mater.* **16** 1038–46

- [164] Kim D, Kim T and Lee Y G 2019 4D printed bifurcated stents with kirigami-inspired structures *J. Vis. Exp.* **2019** 149
- [165] Cabrera M S, Sanders B, Goor O J G M, Driessen-Mol A, Oomens C W J and Baaijens F P T 2017 Computationally designed 3D printed self-expandable polymer stents with biodegradation capacity for minimally invasive heart valve implantation: a proof-of-concept study *3D Print. Addit. Manuf.* **4** 19–29
- [166] Shin Y C et al 2019 Development of a shape-memory tube to prevent vascular stenosis *Adv. Mater.* **31** 1904476
- [167] Ilievski F, Mazzeo A D, Shepherd R F, Chen X and Whitesides G M 2011 Soft robotics for chemists *Angew. Chem., Int. Ed.* **50** 1890–5
- [168] Goole J and Amighi K 2016 3D printing in pharmaceuticals: a new tool for designing customized drug delivery systems *Int. J. Pharm.* **499** 376–94
- [169] Vashist A, Kaushik A, Vashist A, Jayant R D, Tomitaka A, Ahmad S, Gupta Y K and Nair M 2016 Recent trends on hydrogel based drug delivery systems for infectious diseases *Biomater. Sci.* **4** 1535–53
- [170] Fu S, Du X, Zhu M, Tian Z, Wei D and Zhu Y 2019 3D printing of layered mesoporous bioactive glass/sodium alginate sodium alginate scaffolds with controllable dual-drug release behaviors *Biomed. Mater.* **14** 065011
- [171] Lui Y S, Sow W T, Tan L P, Wu Y, Lai Y and Li H 2019 4D printing and stimuli-responsive materials in biomedical aspects *Acta Biomater.* **92** 19–36
- [172] Sun Y and Soh S 2015 Printing tablets with fully customizable release profiles for personalized medicine *Adv. Mater.* **27** 7847–53
- [173] Goyanes A, Robles Martinez P, Buazn A, Basit A W and Gaisford S 2015 Effect of geometry on drug release from 3D printed tablets *Int. J. Pharm.* **494** 657–63
- [174] Wang J, Zhang Y, Aghda N H, Pillai A R, Thakkar R, Nokhodchi A and Maniruzzaman M 2021 Emerging 3D printing technologies for drug delivery devices: current status and future perspective *Adv. Drug Deliv. Rev.* **174** 294–316
- [175] Cui M, Pan H, Su Y, Fang D, Qiao S, Ding P and Pan W 2021 Opportunities and challenges of three-dimensional printing technology in pharmaceutical formulation development *Acta Pharm. Sin. B* **11** 2488–504
- [176] Bellinger A M et al 2016 Oral, ultra-long-lasting drug delivery: application toward malaria elimination goals *Sci. Trans. Med.* **8** 365
- [177] Babae S et al 2019 Temperature-responsive biometamaterials for gastrointestinal applications *Sci. Trans. Med.* **11** eaau858
- [178] Kirtane A R et al 2018 Development of an oral once-weekly drug delivery system for HIV antiretroviral therapy *Nat. Commun.* **9** 2
- [179] Maroni A, Melocchi A, Zema L, Foppoli A and Gazzaniga A 2020 Retentive drug delivery systems based on shape memory materials *J. Appl. Polym. Sci.* **137** 48798
- [180] Firth J, Gaisford S and Basit A W 2018 A new dimension: 4D printing opportunities in pharmaceuticals *AAPS Advances in the Pharmaceutical Sciences Series* vol 31 (Berlin: Springer) pp 153–62
- [181] Durga Prasad Reddy R and Sharma V 2020 Additive manufacturing in drug delivery applications: a review *Int. J. Pharm.* **589** 119820
- [182] Liu X, Zhao K, Gong T, Song J, Bao C, Luo E, Weng J and Zhou S 2014 Delivery of growth factors using a smart porous nanocomposite scaffold to repair a mandibular bone defect *Biomacromolecules* **15** 1019–30
- [183] Melocchi A et al 2019 Expandable drug delivery system for gastric retention based on shape memory polymers: development via 4D printing and extrusion *Int. J. Pharm.* **571** 118700
- [184] Mirani B, Pagan E, Currie B, Siddiqui M A, Hosseinzadeh R, Mostafalu P, Zhang Y S, Ghahary A and Akbari M 2017 An advanced multifunctional hydrogel-based dressing for wound monitoring and drug delivery *Adv. Healthcare Mater.* **6** 19
- [185] Han D, Morde R S, Mariani S, La Mattina A A, Vignali E, Yang C, Barillaro G and Lee H 2020 4D printing of a bioinspired microneedle array with backward-facing barbs for enhanced tissue adhesion *Adv. Funct. Mater.* **30** 1909197
- [186] Ashfaq U A, Riaz M, Yasmeen E and Yousaf M 2017 Recent advances in nanoparticle-based targeted drug-delivery systems against cancer and role of tumor microenvironment *Crit. Rev. Ther. Drug Carrier Syst.* **34** 317–53
- [187] Senapati S, Mahanta A K, Kumar S and Maiti P 2018 Controlled drug delivery vehicles for cancer treatment and their performance *Signal Transduct. Target. Ther.* **3** 7
- [188] Larush L, Kaner I, Fluksman A, Tamsut A, Pawar A A, Lesnovski P, Benny O and Magdassi S 2017 3D printing of responsive hydrogels for drug-delivery systems *J. 3D Print. Med.* **1** 4
- [189] Okwuosa T C, Pereira B C, Arafat B, Cieszyńska M, Isreb A and Alhnan M A 2017 Fabricating a shell-core delayed release tablet using dual FDM 3D printing for patient-centred therapy *Pharm. Res.* **34** 427–37
- [190] Goyanes A, Fina F, Martorana A, Sedough D, Gaisford S and Basit A W 2017 Development of modified release 3D printed tablets (printlets) with pharmaceutical excipients using additive manufacturing *Int. J. Pharm.* **527** 21–30
- [191] Lin G, Makarov D and Schmidt O G 2017 Magnetic sensing platform technologies for biomedical applications *Lab Chip* **17** 1884–912
- [192] Miyashita S, Guitron S, Ludersdorfer M, Sung C R and Rus D 2015 An untethered miniature origami robot that self-folds, walks, swims, and degrades *Proc.—IEEE Int. Conf. on Robotics and Automation (June 2015)* (<https://doi.org/10.1109/ICRA.2015.7139386>)
- [193] Hu Q, Katti P S and Gu Z 2014 Enzyme-responsive nanomaterials for controlled drug delivery *Nanoscale* **6** 12273–86
- [194] Wang X, Qin X H, Hu C, Terzopoulou A, Chen X Z, Huang T Y, Maniura-Weber K, Pané S and Nelson B J 2018 3D printed enzymatically biodegradable soft helical microswimmers *Adv. Funct. Mater.* **28** 1804076
- [195] Ceylan H, Yasa I C, Yasa O, Tabak A F, Giltinan J and Sitti M 2019 3D-printed biodegradable microswimmer for theranostic cargo delivery and release *ACS Nano* **13** 3353–62
- [196] Wang Y, Miao Y, Zhang J, Wu J P, Kirk T B, Xu J, Ma D and Xue W 2018 Three-dimensional printing of shape memory hydrogels with internal structure for drug delivery *Mater. Sci. Eng. C* **84** 44–51
- [197] Melocchi A, Inverardi N, Ubaldi M, Baldi F, Maroni A, Pandini S, Briatico-Vangosa F, Zema L and Gazzaniga A 2019 Retentive device for intravesical drug delivery based on water-induced shape memory response of poly(vinyl alcohol): design concept and 4D printing feasibility *Int. J. Pharm.* **559** 299–311
- [198] Agarwal T et al 2021 4D printing in biomedical applications: emerging trends and technologies *J. Mater. Chem. B* **9** 7608–32
- [199] Kim D et al 2021 Review of machine learning methods in soft robotics *PLoS One* **16** e0246102
- [200] Li Y C, Zhang Y S, Akpek A, Shin S R and Khademhosseini A 2017 4D bioprinting: the next-generation technology for biofabrication enabled by stimuli-responsive materials *Biofabrication* **9** 012001
- [201] Rivera-Tarazona L K, Campbell Z T and Ware T H 2021 Stimuli-responsive engineered living materials *Soft Matter* **17** 785–809
- [202] Gilbert C and Ellis T 2019 Biological engineered living materials: growing functional materials with

- genetically programmable properties *ACS Synth. Biol.* **8** 1–15
- [203] Nguyen P Q, Courchesne N-M D, Duraj-Thatte A, Praveschotinunt P and Joshi N S 2018 Engineered living materials: prospects and challenges for using biological systems to direct the assembly of smart materials *Adv. Mater.* **30** e1704847
- [204] Liu S and Xu W 2020 Engineered living materials-based sensing and actuation *Front. Sens.* **1** 586300
- [205] Gilbert C, Tang T-C, Ott W, Dorr B A, Shaw W M, Sun G L, Lu T K and Ellis T 2021 Living materials with programmable functionalities grown from engineered microbial co-cultures *Nat. Mater.* **20** 691–700